

Sparse Group Fused Lasso for Model Segmentation

David Degras

March 21, 2022

Abstract

This article introduces the sparse group fused lasso (SGFL) as a statistical framework for segmenting high dimensional regression models. To compute solutions of the SGFL, a nonsmooth and nonseparable convex program, we develop a hybrid optimization method that is fast, requires no tuning parameter selection, and is guaranteed to converge to a global minimizer. In numerical experiments, the hybrid method compares favorably to state-of-the-art techniques both in terms of computation time and accuracy; benefits are particularly substantial in high dimension. The hybrid method is implemented in the R package `sparseGFL` available on the author's Github page. The SGFL framework, presented here in the context of multivariate time series, can be extended to multichannel images and data collected over graphs.

Keywords: Multivariate time series, model segmentation, high-dimensional regression, convex optimization, hybrid algorithm

1 Introduction

In the analysis of complex signals, using a single statistical model with a fixed set of parameters is rarely enough to track data variations over their entire range. In long and/or high-dimensional time series for example, the presence of nonstationarity, either in the form of slowly drifting dynamics or of abrupt regime changes, requires that statistical models flexibly account for temporal variations in signal characteristics. To overcome the intrinsic limitations of approaches based on a single model vis-à-vis heterogeneous and nonstationary signals, *model segmentation* techniques have been successfully employed in various fields including image processing (Alaíz et al., 2013; Friedman et al., 2007) genetics (Bleakley and Vert, 2011; Tibshirani and Wang, 2007), brain imaging (Beer et al., 2019; Xu and Lindquist, 2015), finance Hallac et al. (2019); Nystrup et al. (2017), industrial monitoring (Saxén et al., 2016), oceanography (Ranalli et al., 2018), seismology (Ohlsson et al., 2010), and ecology (Alewijns et al., 2018). Model segmentation consists in partitioning the domain of the signal (e.g. the temporal range of a time series or the lattice of a digital

image) into a small number of segments or regions such that for each segment, the data are suitably represented with a single model. The models used to segment the data are typically of the same type (e.g. linear model) but differ by their parameters. The task of model segmentation is closely related to *change point detection* and is commonly referred to as (hybrid or time-varying) system identification in the engineering literature.

This work considers model segmentation in the following setup:

- *Structured multivariate data.* The observed data are multivariate predictor and response variables measured over a time grid, spatial lattice, or more generally a graph.
- *Regression.* Predictor and response variables are related through a regression model, e.g. a linear model, generalized linear model, or vector autoregressive model.
- *High dimension.* There are far more predictors than response variables. However, at each measurement point, the responses only depend on a small number of predictors.

For simplicity, we present our methods and results in the context of linear regression with time series data, keeping in mind that our work readily extends to other regression models and graph structures. Let $(X_t)_{1 \leq t \leq T}$ and $(y_t)_{1 \leq t \leq T}$ be multivariate time series where $y_t \in \mathbb{R}^d$ is a response vector and $X_t \in \mathbb{R}^{d \times p}$ a predictor matrix. We consider the time-varying multivariate linear model $y_t = X_t \beta_t + \varepsilon_t$, where $\beta_t \in \mathbb{R}^p$ is an unknown regression vector and ε_t a random vector with mean zero. As noted above, we assume that $p \gg d$, that the β_t are sparse, and that $\beta_t = \beta_{t+1}$ for most values of t , that is, $\beta = (\beta_t)_{1 \leq t \leq T}$ is a piecewise constant function of t with few change points. Our goal is to develop efficient computational methods for estimating β and its change points $t : \beta_{t-1} \neq \beta_t$.

Before introducing the optimization problem at the core of this study, namely the *sparse group fused lasso* (SGFL), we review relevant work on model segmentation, change point detection, and structured sparse regression.

Related work

We first introduce some notations. Throughout the paper, $\|\cdot\|_q$ denotes the standard ℓ_q norm: $\|x\|_q = (\sum_{i=1}^n |x_i|^q)^{1/q}$ if $0 < q < \infty$ and $\|x\|_\infty = \max_{1 \leq i \leq n} (|x_i|)$ if $q = \infty$ for $x \in \mathbb{R}^n$. For convenience, we use the same notation $\beta = (\beta_1, \dots, \beta_T)$ to refer to regression coefficients either as a single vector in \mathbb{R}^{pT} or as a sequence of T vectors in \mathbb{R}^p .

Combinatorial approaches to change point detection There is an extensive literature on change point detection spanning multiple fields and decades, which we only very partially describe here. For estimating changes in linear regression models, if the number $K \geq 2$ of segments (or equivalently the number $K - 1$ of change points) is fixed, the

segmentation problem can be expressed as

$$\min_{\substack{(\beta_1, \dots, \beta_K) \in \mathbb{R}^{pK} \\ 1 < T_1 < \dots < T_{K-1} \leq T}} \frac{1}{2} \sum_{k=1}^K \sum_{t=T_{k-1}}^{T_k-1} \|y_t - X_t \beta_k\|_2^2 \quad (1)$$

with $T_0 = 1$ and $T_K = T + 1$. For a given set of change points (T_1, \dots, T_{K-1}) , the minimizing argument $\beta = (\beta_1, \dots, \beta_K)$ and associated objective value are obtained by ordinary least squares regression. Accordingly the optimization reduces to a combinatorial problem solvable by dynamic programming (Bai and Perron, 2003). This technique is computationally demanding as it requires performing $O(T^2)$ linear regressions before carrying out the dynamic program per se; the time spent in linear regression can however be reduced through recursive calculations. A fundamental instance of model segmentation in (1) occurs when the design matrix X_t is the identity matrix. In this case the problem is to approximate the signal (y_t) itself with a piecewise constant function.

If K is not prespecified, one may add a penalty function to (1) so as to strike a compromise between fitting the data and keeping the model complexity low. Examples of penalty functions on K include the Akaike Information Criterion (AIC), Bayes Information Criterion (BIC), as well as more recent variants for high-dimensional data (Yao, 1988; Chen and Chen, 2008). Another way to select K is to add/remove change points based on statistical tests or other criteria in top/down or bottom/up approaches. See Basseville and Nikiforov (1993) for a classical book on statistical change point detection and Truong et al. (2018) for a more recent survey. Readers interested in the popular method of binary segmentation may also consult Bai (1997); Fryzlewicz (2014); Leonardi and Bühlmann (2016).

Total variation penalty methods Studying the piecewise constant approximation of 1-D signals, Friedman et al. (2007) utilize a convex relaxation of (1) called the *fused lasso signal approximation* (FLSA):

$$\min_{\beta \in \mathbb{R}^T} \frac{1}{2} \sum_{t=1}^T (y_t - \beta_t)^2 + \lambda_1 \sum_{t=1}^T |\beta_t| + \lambda_2 \sum_{t=1}^{T-1} |\beta_{t+1} - \beta_t|. \quad (2)$$

Here, hard constraints or penalties on the number K of segments are replaced by a penalty on the increments $\beta_{t+1} - \beta_t$. This total variation penalty promotes flatness in the profile of β , that is, a small number of change points. The ℓ_1 penalty on β , called a *lasso penalty* in the statistical literature, favors sparsity in β . The regularization parameters $\lambda_1, \lambda_2 > 0$ determine a balance between fidelity to the data, sparsity of β , and number of change points. They can be specified by the user or selected from the data, for example by cross-validation. Friedman et al. (2007) derive an efficient coordinate descent method to calculate the solution $\hat{\beta} = \hat{\beta}(\lambda_1, \lambda_2)$ to (2) along a path of values of (λ_1, λ_2) . Their method can also

be applied to the more general problem of *fused lasso regression*

$$\min_{\beta \in \mathbb{R}^T} \frac{1}{2} \sum_{i=1}^n (y_i - x'_i \beta)^2 + \lambda_1 \sum_{t=1}^T |\beta_t| + \lambda_2 \sum_{t=1}^{T-1} |\beta_{t+1} - \beta_t| \quad (3)$$

where $x_i \in \mathbb{R}^T$ is a vector of predictors, although it is not guaranteed to yield a global minimizer in this case. One may recover the FLSA (2) by setting $n = T$ and taking the x_i as the canonical basis of \mathbb{R}^T in (3). More recent approaches to fused lasso regression include Hoeffling (2010); Liu et al. (2010); Wang et al. (2015).

The FLSA and fused lasso can easily be adapted to the multivariate setup as follows:

$$\min_{\beta \in \mathbb{R}^{pT}} \frac{1}{2} \sum_{t=1}^T \|y_t - X_t \beta_t\|_2^2 + \lambda_1 \sum_{t=1}^T \|\beta_t\|_1 + \lambda_2 \sum_{t=1}^{T-1} \|\beta_{t+1} - \beta_t\|_1 \quad (4)$$

where $X_t \in \mathbb{R}^{d \times p}$, $y_t \in \mathbb{R}^d$, and $\beta = (\beta_1, \dots, \beta_T)$. These approaches are however not suitable for segmenting multivariate signals/models as they typically produce change points that are only shared by few predictor variables. This is because the ℓ_1 norm in the total variation penalty affects each of the p predictors separately. A simple way to induce change points common to all predictors is to replace this ℓ_1 norm by an ℓ_q norm with $q > 1$. Indeed for $q > 1$, the ℓ_q norm of \mathbb{R}^p is differentiable everywhere except at the origin, which promotes $\|\beta_{t+1} - \beta_t\|_q = 0$. Typically, for the model estimate to have a change point at time $t + 1$, a jump of at least modest size must occur in a significant fraction of the p time-varying regression coefficients between t and $t + 1$. Due to its computational simplicity, the ℓ_2 norm is often used in practice. For example, a common approach to denoising multivariate signals is to solve

$$\min_{\beta \in \mathbb{R}^{dT}} \frac{1}{2} \sum_{t=1}^T \|y_t - \beta_t\|_2^2 + \lambda_2 \sum_{t=1}^{T-1} w_t \|\beta_{t+1} - \beta_t\|_2 \quad (5)$$

where the w_t are positive weights. Bleakley and Vert (2011) reformulate this problem as a group lasso regression and apply the group LARS algorithm (see Yuan and Lin, 2006) to efficiently find solution paths $\hat{\beta} = \hat{\beta}(\lambda_2)$ as λ_2 varies. Wytock et al. (2014) propose Newton-type methods for (5) that extend to multichannel images. These two papers refer to problem (5) as the *group fused lasso* (GFL).

To segment multivariate regression models with group sparsity structure, Alaíz et al. (2013) consider a generalization of (5) that they also call group fused lasso:

$$\min_{\beta \in \mathbb{R}^{pT}} \frac{1}{2} \sum_{t=1}^T \|y_t - X_t \beta_t\|_2^2 + \lambda_1 \sum_{t=1}^T \|\beta_t\|_2 + \lambda_2 \sum_{t=1}^{T-1} w_t \|\beta_{t+1} - \beta_t\|_2. \quad (6)$$

They handle the optimization with a proximal splitting method similar to Dykstra’s projection algorithm. Songsiri (2015) studies (6) in the context of vector autoregressive models, using the well-known alternative direction method of multipliers (ADMM). See e.g. Combettes and Pesquet (2011) for an overview of proximal methods and ADMM.

Sparse Group Fused Lasso

Under our assumptions, the set of regression coefficients $\beta = (\beta_1, \dots, \beta_T)$ in the time-varying model $y_t = X_t\beta_t + \varepsilon_t$ is sparse and piecewise constant with few change points. To enforce these assumptions in fitting the model to data, we propose to solve

$$\min_{\beta \in \mathbb{R}^{pT}} F(\beta) := \frac{1}{2} \sum_{t=1}^T \|y_t - X_t\beta_t\|_2^2 + \lambda_1 \sum_{t=1}^T \|\beta_t\|_1 + \lambda_2 \sum_{t=1}^{T-1} w_t \|\beta_{t+1} - \beta_t\|_2. \quad (7)$$

Problem (7) has common elements with the fused lasso (4) and the group fused lasso (6) but the three problems are distinct and not reducible to one another. For example, (4) uses an ℓ_1 TV penalty whereas (7) uses an ℓ_2 TV penalty to promote blockwise equality $\beta_t = \beta_{t+1}$. Also, unlike (6) which exploits an ℓ_2 penalty to induce group sparsity in β , (7) features a standard lasso penalty. To distinguish (7) from the group fused lasso problems (5)-(6), we call it *sparse group fused lasso* (SGFL). (Problem (7) is referred to as ℓ_2 variable fusion in Barbero and Sra (2011) but we have not found this terminology elsewhere in the literature.) The GFL (5) is a special case of (7) where $X_t = I_d$ (identity matrix) for all t and $\lambda_1 = 0$.

Remark 1 (Intercept). *A time-varying intercept vector δ_t can be added to the regression model, yielding $y_t = X_t\beta_t + \delta_t + \varepsilon_t$. While intercepts are typically not penalized in lasso regression, one must assume some sparsity in the increments $\delta_{t+1} - \delta_t$ for the extended model to be meaningful. Accordingly, the extended SGFL expresses as*

$$\begin{aligned} \min_{\beta, \delta} \quad & \frac{1}{2} \sum_{t=1}^T \|y_t - X_t\beta_t - \delta_t\|_2^2 + \lambda_1 \sum_{t=1}^T \|\beta_t\|_1 \\ & + \lambda_2 \sum_{t=1}^{T-1} w_t \sqrt{\|\beta_{t+1} - \beta_t\|_2^2 + \|\delta_{t+1} - \delta_t\|_2^2}. \end{aligned} \quad (8)$$

For simplicity of exposition, we only consider problem (7) in this paper, noting that all methods and results easily extend to (8).

The objective function F in (7) has three components: a smooth function (squared loss), a nonsmooth but separable function (elastic net penalty), and a nonsmooth, nonseparable function (total variation penalty). We recall that a function $f(\beta_1, \dots, \beta_T)$ is said to be

(block-)separable if it can be expressed as a sum of functions $\sum_{t=1}^T f_t(\beta_t)$. All three functions are convex. Accordingly, the SGFL (7) is a *nonsmooth, nonseparable convex program*. Several off-the-shelf methods can be found in the convex optimization literature for this type of problem, among which primal-dual algorithms take a preeminent place (Condat, 2013; Yan, 2018). One could also utilize general-purpose convex optimization tools such as proximal methods (for instance, the Dykstra-like approach of Alaíz et al. (2013) can easily be adapted to (7)), ADMM and its variants, or even subgradient methods. However, these approaches do not take full advantage of the structure of (7), which may cause computational inefficiencies. In addition, these approaches aim at function minimization and not model segmentation or change point detection. As a result, they typically produce solutions for which every time t is a change point and where the task of recovering the “true” underlying change points (or segments) may be nontrivial. By devising customized methods for SGFL, one may expect substantial gains in computational speed while at the same time producing well-defined model segmentations.

Contributions and organization the paper

We make the following contributions with this paper.

1. We introduce the sparse group fused lasso (SGFL) for model segmentation in high dimension and develop a hybrid algorithm that efficiently solves the SGFL. The algorithm produces a sequence of solutions that monotonically decrease the objective function and converge to a global minimizer. It yields exact model segmentations, as opposed to generic optimization methods that only provide approximate segmentations. Importantly, the hybrid algorithm does not require any complicated selection of tuning parameters from the user.
2. A key component of the hybrid algorithm is an iterative soft-thresholding scheme for computing the proximal operator of sums of ℓ_1 and ℓ_2 norms. This scheme, which is shown to converge linearly, is of independent interest and can serve as a building block in other optimization problems.
3. We present numerical experiments that compare our hybrid approach to state-of-the-art optimization methods (ADMM, linearized ADMM, primal-dual methods,...) in terms of computational speed and numerical accuracy. We also illustrate SGFL with an application to air quality monitoring.
4. We implement the hybrid algorithm in the R package `sparseGFL` available at <https://github.com/ddegras/sparseGFL>.

The paper is organized as follows. Section 2 gives an overview of the hybrid algorithm. Section 3 details the calculations involved in each part of the algorithm. Section 4 presents

numerical experiments comparing the proposed algorithm to state-of-the-art approaches; it also illustrate SGFL with air quality data. Section 5 summarizes our results and outlines directions for future research. Appendix A contains a proof of linear convergence for the iterative soft-thresholding scheme used in the algorithm.

2 Algorithm overview

Optimization strategy

The proposed algorithm operates at different levels across iterations or cycles. By order of increasing complexity and generality, the optimization of F in (7) may be conducted with respect to:

1. A single block β_t ;
2. A chain of blocks $(\beta_t, \dots, \beta_{t+k})$ such that $\beta_t = \dots = \beta_{t+k}$ (*fusion chain*);
3. All fusion chains;
4. All blocks.

The rationale for this hybrid optimization is to exploit problem structure for fast calculations while guaranteeing convergence to a global solution. By problem structure, we refer both to the block structure of the regression coefficients $\beta = (\beta_1, \dots, \beta_T)$ and to the piecewise nature of the regression model over the time range $\{1, \dots, T\}$. The first two levels of optimization (single block and single chain) involve block coordinate descent methods that can be implemented very quickly in a serial or parallel fashion. The next level (all fusion chains) involves an *active set* approach: assuming to have identified the optimal model segmentation, the associated fusion chains are fixed and F is minimized with respect to these chains. Denoting by K the number of chains, the dimension of the search space decreases from pT variables to pK where typically $K \ll T$. The first three levels of optimization are not sufficient to guarantee convergence to a global solution: they only establish that (i) the current solution $\hat{\beta}$ is blockwise optimal (Tseng, 2001), i.e. F cannot be further reduced by changing just one block in $\hat{\beta}$, and that (ii) the minimum of F over the current model segmentation has been attained. The fourth level consists in a single iteration of the subgradient method, which is known to converge (albeit very slowly) to a global minimizer of the objective function (e.g. Bertsekas, 2015). Of the four optimization levels, this is the most general and most computationally intensive one.

The general strategy of the hybrid algorithm is to identify the optimal model segmentation as early as possible and then solve the associated reduced problem which involves one block of regression coefficients per segment as opposed to one block per time point. Algorithm

1 starts with block coordinate descent cycles and continues until no further progress, i.e. reduction in F , is possible. It then switches to the second level and performs fusion cycles on single chains until no more progress is realized. If progress has been made in any fusion cycle, the algorithm reverts to block coordinate descent; otherwise, it moves up one level and optimizes with respect to all fusion chains. And so on so forth. At the fourth level, the only instance when no progress can be achieved is when a global minimizer has been attained, in which case the algorithm terminates. The flow of these operations is presented in Algorithm 1, the main algorithm of the paper. We now give an overview of the algorithm at each level.

2.1 Block coordinate descent

The principle of block coordinate descent is to partition the optimization variables into blocks and to optimize the objective function at each iteration with respect to a given block while keeping the other blocks fixed. In the optimization (7), time provides a natural blocking structure. Given a current solution $\hat{\beta} = (\hat{\beta}_1, \dots, \hat{\beta}_T)$ and a time index $t \in \{1, \dots, T\}$, the problem formulates as

$$\min_{\beta_t \in \mathbb{R}^p} F(\hat{\beta}_1, \dots, \hat{\beta}_{t-1}, \beta_t, \hat{\beta}_{t+1}, \dots, \hat{\beta}_T).$$

Eliminating terms in F that do not depend on β_t , this amounts to

$$\min_{\beta_t \in \mathbb{R}^p} \frac{1}{2} \|y_t - X_t \beta_t\|_2^2 + \lambda_1 \|\beta_t\|_1 + \lambda_2 \left(w_{t-1} \|\beta_t - \hat{\beta}_{t-1}\|_2 + w_t \|\hat{\beta}_{t+1} - \beta_t\|_2 \right). \quad (9)$$

To accommodate the cases $t = 1$ and $t = T$, we set $w_0 = w_T = 0$ and $\hat{\beta}_0 = \hat{\beta}_{T+1} = 0_p$.

Problem (9) cannot be solved in closed form. Instead, we solve it using the fast iterative soft-thresholding algorithm (FISTA) of Beck and Teboulle (2009), a proximal gradient method that enjoys the accelerated convergence rate $O(1/n^2)$, with n the number of iterations. This algorithm is described in section 3.1. The application of FISTA to (9) entails calculating the proximal operator of the sum of the lasso and total variation penalties. As a reminder, the proximal operator of a convex function $g : \mathbb{R}^p \rightarrow \mathbb{R}$ is defined by $\text{prox}_g(x) = \arg\min_{y \in \mathbb{R}^p} g(y) + (1/2)\|y - x\|_2^2$. Although the proximal operator of each penalty easily obtains in closed form, determining the proximal operator of their sum is highly nontrivial. For this purpose, we develop an iterative soft-thresholding algorithm described in section 3.2.

The optimization (9) is repeated over a sequence of blocks and the solution $\hat{\beta}$ is updated each time until the objective function F in (7) cannot be further reduced. The order in which the blocks are selected for optimization is called the *sweep pattern*. Common examples of sweep patterns include cyclic (e.g. Tseng, 2001), cyclic permutation, (e.g.

Algorithm 1 Sparse Group Fused Lasso

Input: Starting point $\beta^0 \in \mathbb{R}^{pT}$, regularization parameters $\lambda_1 \geq 0, \lambda_2 \geq 0$, tolerance $\epsilon > 0$

Output: β^n

$progressDescent \leftarrow \mathbf{true}, progressFusion \leftarrow \mathbf{true}$

$n \leftarrow 0$

repeat

while $progressDescent = \mathbf{true}$ **do**

$n \leftarrow n + 1$

 Apply Algorithm 2 to β^{n-1} and output β^n {Block descent}

if $F(\beta^n) \geq (1 - \epsilon)F(\beta^{n-1})$ **then**

$progressDescent \leftarrow \mathbf{false}$

end if

end while

while $progressFusion = \mathbf{true}$ **do**

$n \leftarrow n + 1$

 Apply Algorithm 3 to β^{n-1} and output β^n {Fusion: single chains}

if $F(\beta^n) < (1 - \epsilon)F(\beta^{n-1})$ **then**

$progressDescent \leftarrow \mathbf{true}, progressFusion \leftarrow \mathbf{true}$

else

$progressFusion \leftarrow \mathbf{false}$

end if

end while

if $progressDescent = \mathbf{false}$ **and** $progressFusion = \mathbf{false}$ **then**

$n \leftarrow n + 1$

 Apply Algorithm 5 to β^{n-1} and output β^n {Fusion: all chains}

 Apply Algorithm 4 to β^n and output subgradient $g \in \mathbb{R}^{pT}$

if $g \neq 0_{pT}$ **then**

$n \leftarrow n + 1$

$\alpha^* \leftarrow \arg \min_{\alpha > 0} F(\beta^{n-1} - \alpha g)$

$\beta^n \leftarrow \beta^{n-1} - \alpha^* g$ {Subgradient step}

end if

end if

until $F(\beta^n) \geq (1 - \epsilon)F(\beta^{n-1})$

Nesterov, 2012), and greedy selection (e.g. Li and Osher, 2009). The block coordinate descent is summarized in Algorithm 2.

Algorithm 2 Block Coordinate Descent

Input: $\beta^{n-1} \in \mathbb{R}^{pT}$, sweeping pattern (t_1, \dots, t_T)

Output: $\beta^n \in \mathbb{R}^{pT}$

$\hat{\beta} \leftarrow \beta^{n-1}$

for $t = t_1, t_2, \dots, t_T$ **do**

 Check (15)-(16)-(17) for a simple solution to (9)

if simple solution **then**

$\hat{\beta}_t \leftarrow \hat{\beta}_{t-1}$ or $\hat{\beta}_t \leftarrow \hat{\beta}_{t+1}$ as required

else {FISTA}

 Set $f(\beta_t) = \frac{1}{2} \|y_t - X_t \beta_t\|_2^2$, $g(\beta_t) = \lambda_1 \|\beta_t\|_1 + \lambda_2 (w_{t-1} \|\beta_t - \hat{\beta}_{t-1}\|_2 + w_t \|\hat{\beta}_{t+1} - \beta_t\|_2)$

 Apply Algorithm 4 to $f + g$ with starting point $\hat{\beta}_t$, Lipschitz constant $L = \|X_t' X_t\|_2$, and $\text{prox}_{g/L}$ given by (21)-(22). Output β_t^+

$\hat{\beta}_t \leftarrow \beta_t^+$

end if

$\beta_t^n \leftarrow \hat{\beta}_t$

end for

2.2 Fusion cycle: single chain

Because the total variation penalty in F is nonsmooth and nonseparable, the block coordinate descent can get stuck in points that are blockwise optimal but not globally optimal; see Tseng (2001) for a theoretical justification and Friedman et al. (2007) for an example. To overcome this difficulty, one may constrain two or more consecutive blocks $\beta_t, \beta_{t+1}, \dots$ to be equal and optimize F with respect to their common value while keeping other blocks fixed. This fusion strategy is well suited to segmentation because it either preserves segments or merges them into larger ones. Given a current solution $\hat{\beta} = (\hat{\beta}_1, \dots, \hat{\beta}_T)$, the time range $\{1, \dots, T\}$ is partitioned into segments or fusion chains $C_k = \{t : T_k \leq t < T_{k+1}\}$ ($1 \leq k \leq K$) such that the $\hat{\beta}_{T_k} = \dots = \hat{\beta}_{T_{k+1}-1}$ and that $\hat{\beta}_{T_k} \neq \hat{\beta}_{T_{k+1}}$. By convention we set $T_1 = 1$ and $T_{K+1} = T + 1$. If $K > 1$, T_2, \dots, T_K are the estimated change points of the regression model $y_t = X_t \beta_t + \varepsilon_t$. The algorithm successively optimizes (7) over each fusion chain C_k while enforcing the equality constraint $\beta_{T_k} = \dots = \beta_{T_{k+1}-1}$:

$$\min_{\beta_t \in \mathbb{R}^p} F(\hat{\beta}_1, \dots, \hat{\beta}_{T_k-1}, \beta_t, \dots, \beta_t, \hat{\beta}_{T_{k+1}}, \dots, \hat{\beta}_T)$$

where β_t is repeated $n_k = T_{k+1} - T_k$ times. This works out as

$$\min_{\beta_t \in \mathbb{R}^p} \left\{ \frac{1}{2} \sum_{s=T_k}^{T_{k+1}-1} \|y_s - X_s \beta_t\|_2^2 + \lambda_1 n_k \|\beta_t\|_1 \right. \\ \left. + \lambda_2 \left(w_{T_k-1} \|\beta_t - \hat{\beta}_{T_k-1}\|_2 + w_{T_{k+1}} \|\beta_t - \hat{\beta}_{T_{k+1}}\|_2 \right) \right\}. \quad (10)$$

The algorithm may also try to merge two consecutive fusion chains to form a larger chain. To be precise, as t follows a given sweeping pattern t_1, \dots, t_T , the algorithm either: (i) solves (10) if $t = T_k$ and $T_{k+1} - T_k > 1$ (start of a non-singleton chain), (ii) solves (10) with each T_{k+1} replaced by T_{k+2} and n_k by $n_k + n_{k+1}$ if $t = T_{k+1} - 1$ and $t < T$ (end of a chain), or (iii) skips to the next value of t in other cases. The optimization (10) is performed in the same way as the block coordinate descent (9) (FISTA + iterative soft-thresholding). The fusion cycle for single chains is summarized in Algorithm 3.

2.3 Fusion cycle: all chains

When no further reduction can be achieved in F by changing a single block or single fusion chain in the current solution $\hat{\beta} \in \mathbb{R}^{pT}$, a logical next step is to optimize F with respect to *all* fusion chains. Specifically, one identifies the fusion chains $C_k = \{t : T_k \leq t < T_{k+1}\}$ ($1 \leq k \leq K$) over which $\hat{\beta} = (\hat{\beta}_t)$ is constant and optimizes F with respect to all blocks β_t under the equality constraints induced by the fusion chains:

$$\min_{\beta_{T_1}, \dots, \beta_{T_K} \in \mathbb{R}^p} F(\beta_{T_1}, \dots, \beta_{T_1}, \dots, \beta_{T_K}, \dots, \beta_{T_K})$$

with each β_{T_k} repeated $n_k = T_{k+1} - T_k$ times. Explicitly, this amounts to

$$\min_{\beta_{T_1}, \dots, \beta_{T_K}} \left\{ \frac{1}{2} \sum_{k=1}^K \sum_{t=T_k}^{T_{k+1}-1} \|y_t - X_t \beta_{T_k}\|_2^2 + \lambda_1 \sum_{k=1}^K n_k \|\beta_{T_k}\|_1 \right. \\ \left. + \lambda_2 \sum_{k=1}^{K-1} w_{T_{k+1}-1} \|\beta_{T_{k+1}} - \beta_{T_k}\|_2 \right\}. \quad (11)$$

To solve (11) we employ a version of FISTA slightly different from the one used in (9) and (10). In particular this version (Algorithm 5) operates under the requirement that $\beta_{T_k} \neq \beta_{T_{k+1}}$ for all k . If two blocks β_{T_k} and $\beta_{T_{k+1}}$ become equal during the optimization, the corresponding fusion chains C_k and C_{k+1} are merged and problem (11) is restarted. Details are given in section 3.3.

Algorithm 3 Fusion Cycle: Single Chain

Input: $\beta^{n-1} \in \mathbb{R}^{pT}$, sweeping pattern (t_1, \dots, t_T)

Output: β^n

$\hat{\beta} \leftarrow \hat{\beta}^{n-1}$

Determine fusion chains C_1, \dots, C_K and chain starts $T_1 \leq \dots \leq T_K$

for $t = t_1, t_2, \dots, t_T$ **do**

if $t = T_k$ for some k and $T_{k+1} - T_k > 1$ **then** {chain start}

$a \leftarrow T_k, \quad b \leftarrow T_{k+1} - 1$

else if $t = T_{k+1} - 1$ for some $k < K$ **then** {chain end}

$a \leftarrow T_k, \quad b \leftarrow T_{k+2} - 1$

else {chain interior}

 Skip to next t

end if

 Set $f(\beta_t) = \frac{1}{2} \sum_{s=a}^b \|y_s - X_s \beta_t\|_2^2$

 Set $g(\beta_t) = \lambda_1(b - a + 1)\|\beta_t\|_1 + \lambda_2(w_{a-1}\|\beta_t - \hat{\beta}_{a-1}\|_2 + w_b\|\hat{\beta}_{b+1} - \beta_t\|_2)$

 Check (24)-(25)-(26) for a simple solution to $\min(f + g)$

if simple solution **then**

$\beta_t^+ \leftarrow \hat{\beta}_{a-1}$ or $\beta_t^+ \leftarrow \hat{\beta}_{b+1}$ as required

else {FISTA}

 Apply Algorithm 4 to $f + g$ with starting point $\hat{\beta}_t$, Lipschitz constant $L = \|\sum_{s=a}^b X_s' X_s\|_2$, and $\text{prox}_{g/L}$ given by (27). Output β_t^+

end if

$\beta^+ \leftarrow (\hat{\beta}_1, \dots, \hat{\beta}_{a-1}, \beta_t^+, \dots, \beta_t^+, \hat{\beta}_{b+1}, \dots, \hat{\beta}_T) \in \mathbb{R}^{pT}$

if $b = T_{k+2} - 1$ and $F(\beta^+) < F(\hat{\beta})$ **then** {merge C_k and C_{k+1} }

 Remove T_{k+1} from $\{T_1, \dots, T_K\}$, set $K \leftarrow K - 1$, relabel chain starts as $T_1 \leq \dots \leq T_K$, and set $T_{K+1} \leftarrow T + 1$

end if

$\hat{\beta}_s \leftarrow \beta_t^+$ and $\beta_s^n \leftarrow \beta_t^+$ for $T_k \leq s < T_{k+1}$

end for

2.4 Checking the optimality of a solution

A vector $x \in \mathbb{R}^n$ ($n \geq 1$) minimizes a convex function $f : \mathbb{R}^n \rightarrow \mathbb{R}$ if and only if 0_n is a *subgradient* of f at x . (The concept of subgradient generalizes the gradient to possibly nondifferentiable convex functions.) This expresses equivalently as the membership of 0_n to the *subdifferential* $\partial f(x)$, that is, the set of all subgradients of f at x . Definition, basic properties, and examples of subgradients and subdifferentials can be found in textbooks on convex analysis, e.g. Rockafellar (2015).

In order to formulate the optimality conditions of the SGFL problem (7), we define the sign operator

$$\text{sgn}(x) = \begin{cases} \{1\} & \text{if } x > 0, \\ \{-1\} & \text{if } x < 0, \\ [-1, 1] & \text{if } x = 0, \end{cases}$$

for $x \in \mathbb{R}$ and extend it as a set-valued function from \mathbb{R}^n to \mathbb{R}^n in a componentwise fashion: $(\text{sgn}(x))_i = \text{sgn}(x_i)$ ($1 \leq i \leq n$). Now, a vector $\hat{\beta} = (\hat{\beta}_1, \dots, \hat{\beta}_T) \in \mathbb{R}^{pT}$ minimizes F if and only if 0_{pT} is a subgradient at $\hat{\beta}$, that is, if and only if there exist vectors $u_1, \dots, u_T \in \mathbb{R}^p$ and $v_1, \dots, v_{T-1} \in \mathbb{R}^p$ satisfying

$$X'_t(X_t \hat{\beta}_t - y_t) + \lambda_1 u_t + \lambda_2 (w_{t-1} v_{t-1} - w_t v_t) = 0_p \quad (12a)$$

and

$$u_t \in \text{sgn}(\hat{\beta}_t) \quad (12b)$$

for $1 \leq t \leq T$ as well as

$$\begin{cases} v_t = \frac{\hat{\beta}_{t+1} - \hat{\beta}_t}{\|\hat{\beta}_{t+1} - \hat{\beta}_t\|_2} & \text{if } \hat{\beta}_t \neq \hat{\beta}_{t+1}, \\ \|v_t\|_2 \leq 1 & \text{if } \hat{\beta}_t = \hat{\beta}_{t+1}, \end{cases} \quad (12c)$$

for $1 \leq t \leq T-1$. By convention we take $v_0 = v_T = 0_p$. Conditions (12b)-(12c) arise from the facts that the subdifferential of the ℓ_1 norm is the sign operator and that the subdifferential of the ℓ_2 norm at 0_p is the ℓ_2 -unit ball of \mathbb{R}^p .

The optimality conditions (12a)-(12b)-(12c) can be checked by solving

$$\min_{U \in \mathcal{C}_1, V \in \mathcal{C}_2} \frac{1}{2} \|Z + \lambda_1 \alpha U + \lambda_2 V W D'\|_F^2 \quad (13)$$

where $U = (u_1, \dots, u_T) \in \mathbb{R}^{p \times T}$, $V = (v_1, \dots, v_{T-1}) \in \mathbb{R}^{p \times (T-1)}$, $Z = (z_1, \dots, z_T) \in \mathbb{R}^{p \times T}$ with $z_t = X'_t(X_t \hat{\beta}_t - y_t) + \lambda_1(1 - \alpha)\hat{\beta}_t$, and $D \in \mathbb{R}^{T \times (T-1)}$ is the differencing matrix given by $(D)_{ij} = -1$ if $i = j$, $(D)_{ij} = 1$ if $i = j+1$, and $(D)_{ij} = 0$ otherwise. (Here we use matrix formalism to express (12a) more simply.) The sets \mathcal{C}_1 and \mathcal{C}_2 embody the constraints (12b)

and (12c), respectively. If the minimum of (13) is zero, then 0_{pT} is a subgradient of F at $\hat{\beta}$ and $\hat{\beta}$ minimizes F . In this case the optimization is over.

A closer examination of (12a)-(12b)-(12c) reveals that change points in $\hat{\beta}$ break the global problem (13) into independent subproblems. More precisely, let $T_2 < \dots < T_K$ be the change points induced by $\hat{\beta}$ (assuming there is at least one) and C_1, \dots, C_K the associated segmentation of $\{1, \dots, T\}$. The constraints (12c) entirely determine the vectors v_{T_k-1} ($k \geq 2$), which breaks the coupling of the v_t separated by change points in (12a). On the other hand the constraints (12b) clearly affect each block u_t separately. Therefore, problem (13) can be solved separately (and in parallel) on each fusion chain C_k . We tackle (13) on each C_k using *gradient projection*. We embed this method inside FISTA for faster convergence. The necessary gradient calculation and projections on \mathcal{C}_1 and \mathcal{C}_2 are described in section 3.4.

2.5 Subgradient step

If the attained minimum in (13) is greater than zero, then $\hat{\beta}$ is not a minimizer of F . By design of Algorithm 1 this implies that the segmentation C_1, \dots, C_K associated with $\hat{\beta}$ is suboptimal and that, starting from $\hat{\beta}$, F cannot be further reduced at the first three levels of optimization. In this case, arguments (U^*, V^*) that minimize (13) provide a subgradient $G = Z + \lambda_1 \alpha U^* + \lambda_2 V^* W D'$ of minimum norm. Denoting the vectorized version of G by $g \in \mathbb{R}^{pT}$, the opposite of g is a direction of steepest descent for F at $\hat{\beta}$ (e.g. Shor, 1985). Accordingly, at the fourth level of optimization, the algorithm takes a step in the direction $-g$ with step length obtained by exact line search. The updated solution expresses as $\beta^+ = \hat{\beta} - \alpha^* g$ where $\alpha^* = \operatorname{argmin}_{\alpha > 0} F(\hat{\beta} - \alpha g)$. The subgradient step accomplishes two important things: first, it moves the optimization away from the suboptimal segmentation C_1, \dots, C_K and second, by reducing the objective, it ensures that this segmentation will not be visited again later in the optimization. This is because Algorithm 1 is a descent method and the best solution $\hat{\beta}$ for the segmentation C_1, \dots, C_K has already been attained in a previous cycle of optimization – otherwise the optimality check and subgradient step would not have been performed. Since there is a finite number of segmentations of $\{1, \dots, T\}$, Algorithm 1 eventually finds an optimal segmentation and an associated minimizer of F through the third level of optimization.

Theorem 1. *For any starting point $\beta^0 \in \mathbb{R}^{pT}$, the sequence $(\beta^n)_{n \geq 0}$ generated by Algorithm 1 converges to a (global) minimizer β^* of F .*

3 Computations

This section gives a detailed account of how optimization is carried out at each level (single block, single fusion chain, all fusion chains, all blocks) in Algorithm 1. We first present the fast iterative soft-thresholding algorithm (FISTA) of Beck and Teboulle (2009) which we extensively use in Algorithm 1.

3.1 FISTA

Beck and Teboulle Beck and Teboulle (2009) consider the convex program

$$\min_{x \in \mathbb{R}^n} \{f(x) + g(x)\}$$

where $f : \mathbb{R}^n \rightarrow \mathbb{R}$ is a smooth convex function and $g : \mathbb{R}^n \rightarrow \mathbb{R}$ is a continuous convex function, possibly nonsmooth. The function f is assumed to be differentiable with Lipschitz-continuous gradient:

$$\|\nabla f(x) - \nabla f(y)\|_2 \leq L \|x - y\|_2$$

for all $x, y \in \mathbb{R}^n$ and some finite Lipschitz constant $L > 0$. The function g is assumed to be proximable, that is, its proximal operator $\text{prox}_{\gamma g}(x) = \arg \min_{y \in \mathbb{R}^n} \{g(y) + 1/(2\gamma) \|y - x\|^2\}$ should be easy to calculate for all $\gamma > 0$.

FISTA is an iterative method that replaces at each iteration the difficult optimization of the objective $f + g$ by the simpler optimization of a quadratic approximation Q_L . Given a suitable vector $y \in \mathbb{R}^n$, the goal is to minimize

$$Q_L(x, y) = f(y) + \nabla f(y)'(x - y) + g(x) + \frac{L}{2} \|x - y\|_2^2. \quad (14)$$

with respect to $x \in \mathbb{R}^n$. With a few algebraic manipulations and omitting irrelevant additive constants, Q_L can be rewritten as

$$Q_L(x, y) = g(x) + \frac{L}{2} \left\| x - \left(y - \frac{1}{L} \nabla f(y) \right) \right\|_2^2$$

so that $\arg \min_x Q(x, y) = \text{prox}_{g/L}(y - (1/L)\nabla f(y))$. In other words, the minimization of Q_L is achieved through a gradient step with respect to f followed by a proximal step with respect to g . FISTA can thus be viewed as a proximal gradient method, also known as forward-backward method (e.g. Combettes and Pesquet, 2011). Observing that $Q_L(\cdot, y)$ majorizes $f + g$, FISTA can also be viewed as a majorization-minimization method.

Proximal gradient methods are not new: they have been used for decades. The innovation of FISTA is to accelerate the convergence of standard proximal gradient methods by introducing an auxiliary sequence (y^k) such that y^k is a well-chosen linear combination of x^{k-1} and x^k , the main solution iterates. With this technique, the convergence rate of proximal gradient improves from $O(1/k)$ to $O(1/k^2)$. Algorithm 4 presents FISTA in the case where a Lipschitz constant L is prespecified and kept constant through iterations. Algorithm 5 presents FISTA in the case where L is difficult to determine ahead of time and is chosen by backtracking at each iteration. This version of FISTA requires an initial guess L^0 for the Lipschitz constant as well as a factor $\eta > 1$ by which to increase the candidate value L in backtracking steps.

Algorithm 4 FISTA with constant step size

Input: $x^0 \in \mathbb{R}^n$, Lipschitz constant $L > 0$

Output: x^k

```

 $y^1 \leftarrow x^0, \alpha_1 \leftarrow 1$ 
for  $k = 1, 2, \dots$  do
   $x^k \leftarrow \text{prox}_{g/L} \left( y^k - \frac{1}{L} \nabla f(y^k) \right)$ 
   $\alpha_{k+1} \leftarrow \frac{1 + \sqrt{1 + 4(\alpha_k)^2}}{2}$ 
   $y^{k+1} \leftarrow x^k + \left( \frac{\alpha_k - 1}{\alpha_{k+1}} \right) (x^k - x^{k-1})$ 
end for

```

Algorithm 5 FISTA with backtracking

Input: $x^0 \in \mathbb{R}^n$, $L^0 > 0$, $\eta > 1$

Output: x^k

```

 $y^1 \leftarrow x^0, \alpha_1 \leftarrow 1$ 
for  $k = 1, 2, \dots$  do
   $i \leftarrow 0$ 
  repeat
     $L \leftarrow \eta^i L^{k-1}$ 
     $x^k \leftarrow \text{prox}_{g/L} \left( y^k - (1/L) \nabla f(y^k) \right)$ 
     $i \leftarrow i + 1$ 
  until  $(f + g)(x^k) \leq Q_L(x^k, y^k)$ 
   $L^k \leftarrow L$ 
   $\alpha_{k+1} \leftarrow \frac{1 + \sqrt{1 + 4(\alpha_k)^2}}{2}$ 
   $y^{k+1} \leftarrow x^k + \left( \frac{\alpha_k - 1}{\alpha_{k+1}} \right) (x^k - x^{k-1})$ 
end for

```

3.2 Iterative soft-thresholding

In this section we present a novel iterative soft-thresholding algorithm for computing the proximal operators required in the application of FISTA to problems (9) and (10). We first examine the case of (9) (block coordinate descent) and then show how to adapt the algorithm to (10) (optimization of F with respect to a single fusion chain). Of crucial importance is the soft-thresholding operator

$$S(x, \lambda) = \begin{cases} x + \lambda, & \text{if } x < -\lambda, \\ 0, & \text{if } |x| \leq \lambda, \\ x - \lambda, & \text{if } x > \lambda, \end{cases}$$

where $x \in \mathbb{R}$ and $\lambda \geq 0$ is a threshold. This operator accommodates vector arguments $x \in \mathbb{R}^p$ in a componentwise fashion: $(S(x, \lambda))_i = S(x_i, \lambda)$ ($1 \leq i \leq p$).

Checking for simple solutions. It is advantageous to verify whether $\hat{\beta}_{t-1}$ or $\hat{\beta}_{t+1}$ solves (9) before applying FISTA, which is more computationally demanding. The optimality conditions for (9) are very similar to those for the global problem (7), namely (12a)-(12b)-(12c), although of course the conditions for (9) pertain to a single time t . Hereafter we state these conditions in an easily computable form. Let $\phi : \mathbb{R}^p \times \mathbb{R}^p \times \mathbb{R}_+ \rightarrow \mathbb{R}^p$ be defined in a componentwise fashion by

$$(\phi(x, s, \lambda))_i = \begin{cases} x_i + \lambda_i & \text{if } s_i > 0, \\ x_i - \lambda_i & \text{if } s_i < 0, \\ S(x_i, \lambda_i) & \text{if } s_i = 0. \end{cases}$$

If $\hat{\beta}_{t-1} = \hat{\beta}_{t+1}$, this vector solves (9) if and only if

$$\|\phi(X'_t(X_t\hat{\beta}_{t-1} - y_t), \hat{\beta}_{t-1}, \lambda_1)\|_2 \leq \lambda_2(w_{t-1} + w_t). \quad (15)$$

If $\hat{\beta}_{t-1} \neq \hat{\beta}_{t+1}$, $\hat{\beta}_{t-1}$ solves (9) if and only if

$$\left\| \phi\left(X'_t(X_t\hat{\beta}_{t-1} - y_t) + \lambda_2 w_t \frac{\hat{\beta}_{t-1} - \hat{\beta}_{t+1}}{\|\hat{\beta}_{t-1} - \hat{\beta}_{t+1}\|_2}, \hat{\beta}_{t-1}, \lambda_1\right) \right\|_2 \leq \lambda_2 w_{t-1} \quad (16)$$

and $\hat{\beta}_{t+1}$ solves (9) if and only if

$$\left\| \phi\left(X'_t(X_t\hat{\beta}_{t+1} - y_t) + \lambda_2 w_{t-1} \frac{\hat{\beta}_{t+1} - \hat{\beta}_{t-1}}{\|\hat{\beta}_{t+1} - \hat{\beta}_{t-1}\|_2}, \hat{\beta}_{t+1}, \lambda_1\right) \right\|_2 \leq \lambda_2 w_t. \quad (17)$$

Fixed point iteration. After verifying that neither $\hat{\beta}_{t-1}$ nor $\hat{\beta}_{t+1}$ is a solution of (9), we apply Algorithm 4 (FISTA with constant step size) to (9) using the decomposition

$$\begin{cases} f(\beta_t) = \frac{1}{2} \|y_t - X_t \beta_t\|_2^2, \\ g(\beta_t) = \lambda_1 \|\beta_t\|_1 + \lambda_2 (w_{t-1} \|\beta_t - \hat{\beta}_{t-1}\|_2 + w_t \|\beta_t - \hat{\beta}_{t+1}\|_2). \end{cases} \quad (18)$$

The gradient of the smooth component f is $\nabla f(\beta_t) = X_t'(X_t \beta_t - y_t)$ with Lipschitz constant $L_t = \|X_t' X_t\|_2$. The main task is to calculate the proximal operator of g . Given a vector $z_t \in \mathbb{R}^p$, we seek

$$\text{prox}_{g/L_t}(z_t) = \underset{\beta_t \in \mathbb{R}^p}{\text{argmin}} g(\beta_t) + \frac{L_t}{2} \|\beta_t - z_t\|_2^2. \quad (19)$$

The optimality conditions for this problem are

$$0_p \in L_t (\beta_t - z_t) + \lambda_1 \text{sgn}(\beta_t) + \frac{\lambda_2 w_{t-1}}{\|\beta_t - \hat{\beta}_{t-1}\|_2} (\beta_t - \hat{\beta}_{t-1}) + \frac{\lambda_2 w_t}{\|\beta_t - \hat{\beta}_{t+1}\|_2} (\beta_t - \hat{\beta}_{t+1}) \quad (20)$$

or equivalently

$$\begin{aligned} & \left(L_t + \frac{\lambda_2 w_{t-1}}{\|\beta_t - \hat{\beta}_{t-1}\|_2} + \frac{\lambda_2 w_t}{\|\beta_t - \hat{\beta}_{t+1}\|_2} \right) \beta_t \\ & \in \left(L_t z_t + \frac{\lambda_2 w_{t-1} \hat{\beta}_{t-1}}{\|\beta_t - \hat{\beta}_{t-1}\|_2} + \frac{\lambda_2 w_t \hat{\beta}_{t+1}}{\|\beta_t - \hat{\beta}_{t+1}\|_2} \right) - \lambda_1 \alpha \text{sgn}(\beta_t). \end{aligned}$$

Given $\hat{\beta}_{t-1}$, $\hat{\beta}_{t+1}$ and z_t , we define the operator

$$\mathcal{T}(\beta_t) = \frac{S \left(L_t z_t + \frac{\lambda_2 w_{t-1} \hat{\beta}_{t-1}}{\|\beta_t - \hat{\beta}_{t-1}\|_2} + \frac{\lambda_2 w_t \hat{\beta}_{t+1}}{\|\beta_t - \hat{\beta}_{t+1}\|_2}, \lambda_1 \right)}{L_t + \frac{\lambda_2 w_{t-1}}{\|\beta_t - \hat{\beta}_{t-1}\|_2} + \frac{\lambda_2 w_t}{\|\beta_t - \hat{\beta}_{t+1}\|_2}} \quad (21)$$

for $\beta_t \in \mathbb{R}^p \setminus \{\hat{\beta}_{t-1}, \hat{\beta}_{t+1}\}$ and extend it by continuity: $\mathcal{T}(\hat{\beta}_{t-1}) = \hat{\beta}_{t-1}$ and $\mathcal{T}(\hat{\beta}_{t+1}) = \hat{\beta}_{t+1}$. The optimality conditions (20) now express as the fixed point equation

$$\mathcal{T}(\beta_t) = \beta_t.$$

The operator \mathcal{T} admits the fixed points $\hat{\beta}_{t-1}$, $\hat{\beta}_{t+1}$, and $\text{prox}_{g/L_t}(z_t)$. It can be shown that if $\text{prox}_{g/L_t}(z_t) \notin \{\hat{\beta}_{t-1}, \hat{\beta}_{t+1}\}$, the fixed points $\hat{\beta}_{t-1}$ and $\hat{\beta}_{t+1}$ are *repulsive* in the sense that there exist $\eta, \epsilon > 0$ such that $\|\mathcal{T}(\beta_t) - \hat{\beta}_{t-1}\|_2 \geq (1 + \epsilon) \|\beta_t - \hat{\beta}_{t-1}\|_2$ for $\|\beta_t - \hat{\beta}_{t-1}\|_2 \leq \eta$ (same for $\hat{\beta}_{t+1}$). This suggests calculating $\text{prox}_{g/L_t}(z_t)$ with the iterative soft-thresholding

$$\beta_t^{n+1} = \mathcal{T}(\beta_t^n). \quad (22)$$

Remark 2 (proximal gradient). *The fixed point iteration (21)-(22) can be viewed as a proximal gradient algorithm. Writing $g_1(\beta_t) = \lambda_1 \|\beta_t\|_1$ and $g_2(\beta_t) = \lambda_2 w_{t-1} \|\beta_t - \hat{\beta}_{t-1}\|_2 + \lambda_2 w_t \|\beta_t - \hat{\beta}_{t+1}\|_2 + (L_t/2) \|\beta_t - z_t\|_2^2$, it holds that*

$$\mathcal{T}(\beta_t) = \text{prox}_{\gamma g_1}(\beta_t - \gamma \nabla g_2(\beta_t)) \quad \text{with} \quad \frac{1}{\gamma} = L_t + \frac{\lambda_2 w_{t-1}}{\|\beta_t - \hat{\beta}_{t-1}\|_2} + \frac{\lambda_2 w_t}{\|\beta_t - \hat{\beta}_{t+1}\|_2}. \quad (23)$$

Remark 3 (Weiszfeld's algorithm). *The fixed point iteration (21)-(22) is related in spirit to Weiszfeld's algorithm (Weiszfeld and Plastria, 2009) and its generalizations (e.g. Kuhn, 1973) for the Fermat-Weber location problem $\arg \min_{y \in \mathbb{R}^p} \sum_{i=1}^m w_i \|y - x_i\|_2$, where $x_1, \dots, x_m \in \mathbb{R}^p$ and $w_1, \dots, w_m > 0$ are weights. Weiszfeld's algorithm, in its generalized version, has iterates of the form*

$$y^{n+1} = \left(\sum_{i=1}^m \frac{w_i x_i}{\|y^n - x_i\|_2} \right) / \left(\sum_{i=1}^m \frac{w_i}{\|y^n - x_i\|_2} \right)$$

and is derived along the same lines as (21)-(22), namely by equating the gradient to zero and turning this equation into a fixed point equation.

By exploiting a connection to proximal gradient methods (2) and adapting the results of Bredies and Lorenz (2008) to a nonsmooth setting, we can establish the linear convergence of (21)-(22). We defer the proof of this result to section A. For convenience, let us denote the proximal operator $\text{prox}_{g/L_t}(z_t)$ by β_t^* and the associated objective function by $\bar{g}(\beta_t) = g(\beta_t) + (L_t/2) \|\beta_t - z_t\|_2^2$. We also define the distance $r_n = \bar{g}(\beta_t^n) - \bar{g}(\beta_t^*)$ to the minimum of \bar{g} .

Theorem 2. *Assume that $\hat{\beta}_{t-1}$ and $\hat{\beta}_{t+1}$ are not solutions of (9), that $\beta_t^* \notin \{\hat{\beta}_{t-1}, \hat{\beta}_{t+1}\}$, and that the sequence $(\beta_t^n)_{n \geq 0}$ generated by (21)-(22) has its first term satisfying $\bar{g}(\beta_t^0) < \min(\bar{g}(\hat{\beta}_{t-1}), \bar{g}(\hat{\beta}_{t+1}))$. Then the distance $(r_n)_{n \geq 0}$ vanishes exponentially and $(\beta_t^n)_{n \geq 0}$ converges linearly to β_t^* , that is, there exist constants $C > 0$ and $\lambda \in [0, 1)$ such that*

$$\|\beta_t^n - \beta_t^*\|_2 \leq C \lambda^n.$$

The first two assumptions of Theorem 2 ensure that use of the iterative soft-thresholding (21)-(22) is warranted, in other words, that (9) and (19) do not have simple solutions. The condition on the starting point β_t^0 guarantees that the sequence (β_t^n) does not get stuck in $\hat{\beta}_{t-1}$ or $\hat{\beta}_{t+1}$. It is standard for this type of problem, see e.g. Kuhn (1973). In practice this condition is virtually always met by taking the current FISTA iterate as starting point.

Extension to fusion chains. When considering problem (10) over a fusion chain $C = \{t : a \leq t \leq b\}$, the objective decomposes as

$$\begin{cases} f(\beta_t) = \frac{1}{2} \sum_{s=a}^b \|y_s - X_s \beta_t\|_2^2, \\ g(\beta_t) = \lambda_1 n_C \|\beta_t\|_1 + \lambda_2 \left(w_{a-1} \|\beta_t - \hat{\beta}_{a-1}\|_2 + w_b \|\beta_t - \hat{\beta}_{b+1}\|_2 \right), \end{cases}$$

where $n_C = b - a + 1$. The conditions for $\hat{\beta}_{a-1}$ or $\hat{\beta}_{b+1}$ to be simple solutions of (10) are as follows. If $\hat{\beta}_{a-1} = \hat{\beta}_{b+1}$, this vector solves (10) if and only if

$$\left\| \phi \left(\sum_{s=a}^b X'_s (X_s \hat{\beta}_{a-1} - y_s), \hat{\beta}_{a-1}, \lambda_1 \right) \right\|_2 \leq \lambda_2 (w_{a-1} + w_b). \quad (24)$$

If $\hat{\beta}_{a-1} \neq \hat{\beta}_{b+1}$, $\hat{\beta}_{a-1}$ solves (10) if and only if

$$\left\| \phi \left(\sum_{s=a}^b X'_s (X_s \hat{\beta}_{a-1} - y_s) + \lambda_2 w_b \frac{\hat{\beta}_{a-1} - \hat{\beta}_{b+1}}{\|\hat{\beta}_{a-1} - \hat{\beta}_{b+1}\|_2}, \hat{\beta}_{a-1}, \lambda_1 \right) \right\|_2 \leq \lambda_2 w_{a-1} \quad (25)$$

and $\hat{\beta}_{b+1}$ solves (10) if and only if

$$\left\| \phi \left(\sum_{s=a}^b X'_s (X_s \hat{\beta}_{b+1} - y_s) + \lambda_2 w_{a-1} \frac{\hat{\beta}_{b+1} - \hat{\beta}_{a-1}}{\|\hat{\beta}_{b+1} - \hat{\beta}_{a-1}\|_2}, \hat{\beta}_{b+1}, \lambda_1 \right) \right\|_2 \leq \lambda_2 w_b. \quad (26)$$

If there are no simple solutions to (10), we apply Algorithm 4 to $f + g$. The gradient step is given by $\nabla f(\beta_t) = \sum_{s=a}^b X'_s (X_s \beta_t - y_s)$ and its Lipschitz constant $L_C = \|\sum_{s=a}^b X'_s X_s\|_2$. For a given $z_t \in \mathbb{R}^p$, the proximal operator $\text{prox}_{g/L_C}(z_t)$ is calculated by iteratively applying the soft-thresholding operator

$$\mathcal{T}_C(\beta_t) = \frac{S \left(L_C z_t + \frac{\lambda_2 w_{a-1} \hat{\beta}_{a-1}}{\|\beta_t - \hat{\beta}_{a-1}\|_2} + \frac{\lambda_2 w_b \hat{\beta}_{b+1}}{\|\beta_t - \hat{\beta}_{b+1}\|_2}, \lambda_1 n_C \right)}{L_C + \frac{\lambda_2 w_{a-1}}{\|\beta_t - \hat{\beta}_{a-1}\|_2} + \frac{\lambda_2 w_b}{\|\beta_t - \hat{\beta}_{b+1}\|_2}}. \quad (27)$$

3.3 Optimization over all fusion chains

The optimization (11) is carried out by applying Algorithm 5 (FISTA with backtracking) to $\min_{\beta \in \mathbb{R}^{pK}} (f + g)(\beta)$ where

$$\begin{cases} f(\beta) = \frac{1}{2} \sum_{k=1}^K \sum_{t=T_k}^{T_{k+1}-1} \|y_t - X_t \beta_k\|_2^2 + \lambda_2 \sum_{k=1}^{K-1} w_{T_{k+1}-1} \|\beta_{k+1} - \beta_k\|_2, \\ g(\beta) = \lambda_1 \sum_{k=1}^K n_k \|\beta_k\|_1. \end{cases}$$

For notational convenience, we have relabeled the vectors $\beta_{T_1}, \dots, \beta_{T_K}$ of (11) as β_1, \dots, β_K . Observe that f is nondifferentiable at points $\beta = (\beta_1, \dots, \beta_K)$ such that $\beta_k = \beta_{k+1}$ for some k , which violates the smoothness requirements of section 3.1. We can nonetheless apply FISTA until the algorithm either converges to a minimizer of $f + g$ or to a point of nondifferentiability for f . In the latter case, we merge the fusion chains C_k and C_{k+1} associated with the equality $\beta_k = \beta_{k+1}$ and restart FISTA with the reduced set of chains.

To fully specify the FISTA implementation, it remains to characterize the gradient of f and proximal operator of g . The former, wherever it exists, is given by ($1 \leq k \leq K$)

$$\begin{aligned} \frac{\partial f}{\partial \beta_k}(\beta) &= \sum_{t=T_k}^{T_{k+1}-1} X_t'(X_t \beta_k - y_t) + \lambda_2 w_{T_k-1} \frac{\beta_k - \beta_{k-1}}{\|\beta_k - \beta_{k-1}\|_2} \\ &\quad + \lambda_2 w_{T_{k+1}-1} \frac{\beta_k - \beta_{k+1}}{\|\beta_k - \beta_{k+1}\|_2}. \end{aligned} \tag{28}$$

The proximal operator of g performs soft-thresholding by block ($1 \leq k \leq K$):

$$(\text{prox}_{g/L}(\beta))_k = S(\beta_k, \lambda_1 n_k). \tag{29}$$

3.4 Gradient projection method

Here we describe the method of section 2.4 to check the optimality of a solution $\hat{\beta}$. For simplicity, we move the regularization parameters λ_1, λ_2 and diagonal weight matrix W from the objective in (13) to the constraint sets \mathcal{C}_1 and \mathcal{C}_2 . This is done with a simple change of variables.

Gradient step. Writing the objective as $f(U, V) = \frac{1}{2} \|Z + U + VD'\|_F^2$, the gradient of f is given by

$$\frac{\partial f}{\partial U}(U, V) = U + VD' + Z, \quad \frac{\partial f}{\partial V}(U, V) = UD + VD'D + ZD. \tag{30}$$

Therefore a Lipschitz constant L of $\nabla f(U, V)$ can be found by evaluating the spectral norm of the $(2T - 1) \times (2T - 1)$ matrix

$$\begin{pmatrix} I_T & D \\ D' & D'D \end{pmatrix}.$$

Standard calculations show that this matrix has spectral norm $1 + \|D'D\|_2$ and that the eigenvalues of $D'D$ are $\{2(1 - \cos(\frac{(2k-1)\pi}{2p})), 1 \leq k \leq p\}$. Combining these results, one can take $L = 5$.

Projection step. The orthogonal projection $P_{\mathcal{C}_1}(U)$ of $U \in \mathbb{R}^{p \times T}$ on \mathcal{C}_1 is obtained by applying fixed coefficient constraints and clamping values to the interval $[-\lambda_1, \lambda_1]$ where needed. Its coefficients $(1 \leq t \leq T, 1 \leq i \leq p)$ are given by

$$(P_{\mathcal{C}_1}(U))_{it} = \begin{cases} \lambda_1 & \text{if } (\hat{\beta}_t)_i > 0, \\ -\lambda_1 & \text{if } (\hat{\beta}_t)_i < 0, \\ \min(\max((u_t)_i, -\lambda_1), \lambda_1) & \text{if } (\hat{\beta}_t)_i = 0. \end{cases} \quad (31)$$

The orthogonal projection $P_{\mathcal{C}_2}(V)$ of $V \in \mathbb{R}^{p \times (T-1)}$ on \mathcal{C}_2 is obtained by rescaling the columns of V ($1 \leq t < T$) as necessary:

$$(P_{\mathcal{C}_2}(V))_t = \min\left(\frac{\lambda_2 w_t}{\|v_t\|_2}, 1\right) v_t. \quad (32)$$

Writing $I_{\mathcal{C}}$ for the indicator function of a set \mathcal{C} ($I_{\mathcal{C}}(x) = 0$ if $x \in \mathcal{C}$ and $I_{\mathcal{C}}(x) = +\infty$ otherwise) and $g(U, V) = I_{\mathcal{C}_1}(U) + I_{\mathcal{C}_2}(V)$, the constrained problem (13) reformulates as $\min(f + g)$. We can now apply FISTA (Algorithm 4) to solve this problem with the gradient step given by (30) and the Lipschitz constant $L = 5$ and the proximal step $\text{prox}_{g/L}(U, V) = P_{\mathcal{C}_1}(U) + P_{\mathcal{C}_2}(V)$ given by (31)-(32).

4 Numerical experiments

4.1 Simulations

A simulation study was carried out to compare the proposed hybrid approach to SGFL with state-of-the-art optimization methods. The main focus here is on computational speed. Indeed, high-accuracy solutions are not needed in typical applications of SGFL; it is sufficient to correctly identify the optimal model segmentation and the sparsity structure of the minimizer of (7). Two sweeping patterns are examined for the hybrid approach: cyclical (HYB-C) and simple random sampling without replacement (HYB-R).

Benchmark methods

We provide a brief overview of the optimization methods used as benchmarks for the hybrid method. We refer the reader to the articles mentioned below for full details.

- *Smooth proximal gradient* (SPG) (Chen et al., 2012). This method deals with structured penalized regression problems where the penalty term admits a simple dual formulation, for example, group lasso and fused lasso. The idea of SPG is to add quadratic regularization to the dual expression of the penalty and to solve the smooth approximate problem by FISTA (Beck and Teboulle, 2009). In the context of SGFL, the objective (7) is approximated by $\min_{\beta} \max_{\alpha} \{ \frac{1}{2} \sum_t \|X_t \beta_t - y_t\|_2^2 + \lambda_1 \sum_t \|\beta_t\|_1 + \lambda_2 \sum_t (\alpha_t'(\beta_{t+1} - \beta_t) - \mu \|\alpha_t\|_2^2) \}$ where $\beta \in \mathbb{R}^{pT}$, $\alpha \in \mathbb{R}^{p(T-1)}$, $\|\alpha_t\|_2 \leq w_t$ for all t , and $\mu > 0$ is a regularization parameter.
- *Primal-dual method* (PD) (Condat, 2013; Vũ, 2013). This method pertains to the general convex optimization problem $\min_x f(x) + g(x) + (h \circ L)(x)$ where f is a smooth function, g and h are proximable functions, and L is a linear operator. In SGFL, f is taken to be the squared loss, g the lasso penalty, h the mixed $\ell_{2,1}$ norm, and L the first-order differencing operator. At each iteration, the algorithm essentially requires a few matrix-vector multiplications and two easy evaluations of proximal operators: soft-thresholding and projection on ℓ_2 balls.
- *Alternative direction of multipliers method* (ADMM). This widespread optimization method (see e.g. Boyd et al., 2011; Combettes and Pesquet, 2011) is suitable for convex programs of the form $\min_{x,z} f(x) + g(z)$ subject to linear constraints $Ax + Bz + c = 0$. The SGFL problem (7) can be expressed in this form by setting $x = \beta$, f equal to the squared loss plus lasso penalty, and $g(z) = \lambda_2 \sum_t w_t \|z_t\|_2$ where $z_t = \beta_{t+1} - \beta_t$ for all t . ADMM works by forming an augmented Lagrangian function $L_{\rho}(\beta, z, u) = f(\beta) + g(z) + \frac{\rho}{2} \sum_t \|u_t + z_t - (\beta_{t+1} - \beta_t)\|_2^2$ and optimizing it alternatively with respect to β (lasso problem) and to z (projection on ℓ_2 balls), along with closed-form updates of the dual variable u . The regularization parameter $\rho > 0$ must be selected by the user.
- *Linearized ADMM* (LADMM) (Li et al., 2014). This technique is used in instances where one or both of the x - and z - updates in ADMM are computationally expensive. When applying ADMM to (7), one may linearize the squared loss and regularization term $\frac{\rho}{2} \sum_t \|u_t + z_t - (\beta_{t+1} - \beta_t)\|_2^2$ in the augmented Lagrangian L_{ρ} . This replaces the burdensome lasso problem (β -update) by a simple soft-thresholding operation.

Selection of tuning parameters

All the above methods have tuning parameters whose selection is nontrivial. In addition, the numerical performances of these methods are highly sensitive to their tuning parameters. We adopt the following strategies in the simulations.

- SPG. The parameter μ sets an upper bound on the gap between the minima of the original objective and its smooth approximation. However, suitably small values of μ yield unacceptably slow convergence. For this reason, we employ SPG with restarts, starting from a relatively large μ and decreasing it along a logarithmic scale when the algorithm fails to reduce the objective for 100 successive iterations.
- PD. Two proximal parameters τ, σ and a relaxation parameter ρ must be specified. Following the recommendations of the author of Condat (2013) (personal communication), we set $\rho = 1.9$, $\sigma = 0.25(1/\tau - \max_t \|X_t' X_t\|_2)$, and select τ from the grid $\{10^{-6}, 10^{-5}, \dots, 10^6\}$ by trial and error. Specifically, we run 100 iterations of the PD algorithm with $\tau = 10^{-6}$, $\tau = 10^{-5}$, and so on so forth until the best performance over 100 iterations decreases. (The best performance first increases with τ and then decreases).
- ADMM and LADMM. The regularization parameter ρ is selected by trial and error as above (best performance over 100 iterations), but going from large to small values: $\rho = 10^4, 10^3, \dots$

Simulation setup

We consider the piecewise multivariate linear regression model $y_t = X_t \beta_t + \varepsilon_t$ where β_t ($1 \leq t \leq T$) is constant on each segment $C_k = \{t : T_k \leq t < T_{k+1}\}$ ($1 \leq k \leq K$) with $T_k = \frac{(k-1)T}{K} + 1$ and $K = 10$. Two combinations of data dimensions are used: $(d, p, T) = (100, 500, 200)$ for a problem of moderate size (10^4 optimization variables) and $(d, p, T) = (100, 1000, 1000)$ for a larger problem (10^6 variables). Different correlation levels ρ_X in the predictor variables and noise levels σ_ε are examined. The predictors X_t are sampled from a multivariate normal distribution with mean zero, unit variance, and exchangeable correlation structure: $\text{Cor}((X_s)_i, (X_t)_j) = \rho_X$ if $(s, i) \neq (t, j)$ for $1 \leq s, t \leq T$ and $1 \leq i, j \leq p$. Note that correlation occurs both across components and across time. The regression vectors β_{T_k} are first obtained as independent realizations of $N(0_p, I_p)$, after which a fraction $s = 0.9$ of each vector is selected randomly and set to zero. As a result each β_t has sparsity level 0.9. The response vectors y_t are obtained by adding white noise $\varepsilon_t \sim N(0, \sigma_\varepsilon^2 I)$ to $X_t \beta_t$. The regularization parameters λ_1 and λ_2 are taken so that the SGFL solution $\hat{\beta}$ has the same change points and sparsity level as the true β . For each

setup $(d, p, T, \rho_X, \sigma_\varepsilon)$, the simulation (data generation + optimization) is replicated 100 times if $(d, p, T) = (100, 500, 200)$ and 10 times if $(d, p, T) = (100, 1000, 1000)$.

The simulations are realized in the R programming environment (R Core Team, 2019) on an Intel Xeon Gold processor with 64GB RAM and 32 cores (Ubuntu OS). The SPG, PD, ADMM, and LADMM methods are written in C++ using the Armadillo library (Sanderson and Curtin, 2016) and wrapped in R with `RcppArmadillo`. The proposed hybrid approach uses a mix of C++ and R; it is implemented in the R package `sparseGFL`. The package and simulation scripts are available at <https://github.com/ddegras/sparseGFL>. Each simulation is run on a single CPU core without parallelizing the execution of optimization methods.

The SPG, PD, ADMM, and LADMM methods are executed without stopping criterion for a number of iterations sufficient to reach convergence (3000-5000). The SPG uses restarts as described above for 10^4 iterations at most. For the hybrid approach (HYB-C and HYB-R), the tolerance ϵ used in the stopping criterion of Algorithm 1 must be specified, as it determines not only the total number of iterations realized but also the type of optimization realized at each iteration (block coordinate descent, fusion cycle, etc.). It is set to 10^{-6} to reflect the target relative accuracy of the solution to (7). To avoid spending excessive time in low-level optimization, limits are placed on the allowed numbers of successive block-coordinate descent cycles (10) and of fusion cycles for single chains (5). If these numbers are reached, the hybrid algorithm automatically moves up to the next level of optimization (see section 2).

Results

The main performance measure used in the simulation study is the CPU runtime needed to reach a sufficiently accurate solution to (7). We select a target level of 10^{-6} for the relative accuracy of a solution $\hat{\beta} \in \mathbb{R}^{pT}$. That is, we deem a solution $\hat{\beta}$ to be sufficiently accurate if $F(\hat{\beta}) \leq (1 + 10^{-6}) \min_{\beta} F(\beta)$. This level of accuracy is sufficient to guarantee that a solution $\hat{\beta}$ has the same change points and (exactly or very nearly) the same sparsity structure as the minimizer β^* of F . For PD, ADMM, and LADMM, the initial time spent selecting suitable tuning parameters is included in the CPU runtime. (This initial time represents a relatively small fraction of the total runtime.) We point out that it is quite difficult to know good values of the tuning parameters *a priori* and that the performance of these three methods largely depends on their tuning parameters. Badly chosen tuning parameters may lead to excessively slow convergence or, in the other direction, to numerical overflow and divergence. If in a given simulation, an optimization method fails to reach a relative accuracy 10^{-6} , the total runtime of this method is reported.

The runtimes of the methods (to reach relative accuracy 10^{-6}) are summarized in Table 4.1.

SPG is by far the slowest method, taking an order of magnitude more time than all other methods to converge. This method would likely perform better with more sophisticated or more finely tuned restarting rules than the one used here. ADMM is the next slowest method and is not competitive for SGFL because of the need to solve a lasso problem at each iteration. PD and LADMM show comparable runtimes, with a very slight advantage for LADMM on problems of moderate size and a more marked advantage for PD on larger problems. Given that they are generic methods, their speed is quite satisfactory in comparison to the proposed hybrid method which is tailored for SGFL. In all setups, either HYB-C or HYB-R shows the best average runtime. HYB-R is the fastest method in about 56% of all simulations, HYB-C in 30%, LADMM in 9%, and PD in 5%. Unsurprisingly, HYB-R has a more variable runtime than HYB-C because of the additional randomization of the sweeping pattern. Interestingly, HYB-C performs best in the presence of correlation among predictor variables ($\rho_X \in \{0.10, 0.25\}$) whereas HYB-R shows superior performance when $\rho_X = 0$. The fact that HYB-C and HYB-R improve upon PD (the next best method) by respective speedup factors of 40% and 33% in the high-dimensional and correlated setup $p = 1000, T = 1000, \rho_X = 0.25$ is particularly promising for real world applications. See Figure 1 for an illustration.

Table 1: CPU runtime (in seconds) required to solve the SGFL problem (7) with relative accuracy 10^{-6} . Runtimes are averaged across 100 replications if $(d, p, T) = (100, 500, 200)$ and 10 replications if $(d, p, T) = (100, 1000, 1000)$ with standard deviation in parentheses. Best results are indicated in bold.

d	p	T	σ_ε	ρ_X	SPG	PD	HYB-C	HYB-R	ADMM	LADMM
100	500	200	0.00	0.00	225.7 (118.2)	31.7 (0.5)	26.7 (2.0)	22.3 (3.2)	46.7 (1.4)	28.1 (2.7)
100	500	200	0.25	0.00	212.0 (109.4)	31.8 (0.6)	26.3 (2.1)	22.3 (4.2)	46.7 (1.3)	28.4 (3.9)
100	500	200	2.50	0.00	174.8 (64.7)	30.8 (0.7)	27.9 (2.7)	23.1 (4.9)	45.2 (2.6)	27.4 (0.6)
100	500	200	5.00	0.00	210.8 (103.4)	31.5 (0.7)	16.9 (2.3)	17.1 (3.1)	50.8 (26.9)	28.3 (9.8)
100	500	200	0.00	0.10	173.4 (80.0)	35.7 (6.8)	30.8 (5.8)	45.5 (11.2)	51.4 (5.8)	40.7 (3.7)
100	500	200	0.00	0.25	176.1 (87.1)	50.4 (20.8)	38.0 (8.1)	48.2 (14.3)	76.8 (34.5)	52.1 (23.3)
100	500	200	0.25	0.25	177.6 (98.4)	48.6 (18.6)	37.1 (7.4)	48.4 (15.7)	69.4 (29.9)	47.1 (19.9)
100	1000	1000	0.00	0.00	6120.3 (2617.2)	454.0 (1.7)	698.0 (16.2)	373.6 (37.9)	2261.5 (34.5)	971.8 (7.4)
100	1000	1000	0.00	0.25	7435.5 (2827.9)	758.2 (215.9)	458.1 (134.6)	507.7 (186.7)	2384.6 (34.4)	879.0 (101.9)
100	1000	1000	0.25	0.25	6753.9 (1869.0)	657.8 (245.0)	394.8 (111.2)	454.4 (165.8)	2376.3 (52.3)	893.8 (84.6)

We now turn to the accuracy of the methods, keeping in mind that the target accuracy is $F(\hat{\beta}) \leq (1 + 10^{-6}) \min_{\beta} F(\beta)$. Table 4.1 displays the worst-case accuracy of each method in each simulation setup. For a given method and setup, the worst-case accuracy is calculated as the quantile of level 99% of $F(\hat{\beta}) / \min_{\beta} F(\beta) - 1$ across all simulations. Therefore, values inferior to 10^{-6} in the table indicate that the target accuracy is virtually always met. It is important to remember that for HYB-C and HYB-R, the stopping tolerance $\epsilon = 10^{-6}$ is set to achieve the target accuracy level 10^{-6} , not to produce highly accurate solutions. Despite this fact, the worst-case accuracy of HYB-C is well below 10^{-6} in all setups and so

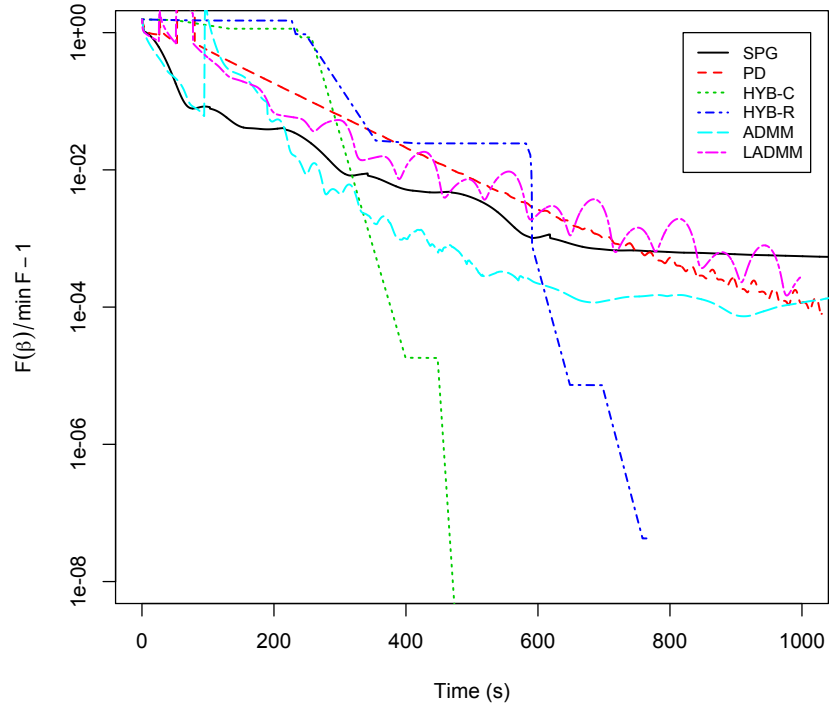


Figure 1: Simulation study: relative accuracy of solution versus CPU runtime in the high-dimensional setup $(d, p, T, \sigma_\varepsilon, \rho_X) = (100, 1000, 1000, 0, 0.25)$ (typical example).

is that of HYB-R (except for the high-noise setup $\sigma_\varepsilon = 5$). No other method achieves the target accuracy so consistently, although they run for a much longer time. Globally, HYB-C meets the target accuracy 10^{-6} in 100% of the simulations, HYB-R in 99.4%, ADMM in 96.2%, PD in 95.8%, LADMM in 95.1%, and SPG in 91.4%.

Table 2: Relative accuracy: worst-case performance. For each method and each setup, the quantile of level 0.99 of $(F(\hat{\beta})/\min_{\beta} F(\beta)) - 1$ across all replications is displayed, where $\hat{\beta}$ is the final estimate produced by the method. For HYB-C and HYB-R, the optimization is stopped whenever the relative decrease in F between two successive iterations is less than 10^{-6} , whereas the other methods run for many iterations without stopping criterion. The numbers in the table should be compared to the target accuracy level 10^{-6} .

d	p	T	σ_ε	ρ_X	SPG	PD	HYB-C	HYB-R	ADMM	LADMM
100	500	200	0.00	0.00	5.7e-06	6.0e-15	1.9e-09	2.0e-09	1.3e-14	3.2e-12
100	500	200	0.20	0.00	8.8e-06	6.0e-15	1.7e-09	1.9e-09	9.1e-15	2.5e-10
100	500	200	2.50	0.00	4.1e-07	5.1e-15	2.6e-07	2.3e-07	6.2e-08	5.8e-09
100	500	200	5.00	0.00	6.6e-07	2.6e-10	7.5e-07	6.3e-04	1.8e-06	5.7e-07
100	500	200	0.00	0.10	6.8e-06	4.4e-07	2.7e-08	4.4e-08	2.7e-10	6.2e-10
100	500	200	0.00	0.25	2.0e-06	3.6e-04	3.1e-07	6.5e-07	2.3e-06	2.0e-05
100	500	200	0.25	0.25	5.6e-06	3.9e-04	2.2e-07	2.3e-07	1.2e-06	3.5e-05
100	1000	1000	0.00	0.00	8.1e-06	0.0e+00	1.8e-10	2.9e-10	1.3e-05	1.9e-06
100	1000	1000	0.00	0.25	5.9e-06	2.8e-04	9.6e-08	8.7e-07	3.3e-05	4.2e-04
100	1000	1000	0.25	0.25	5.3e-06	8.7e-04	1.7e-07	6.3e-08	2.3e-05	8.3e-05

4.2 Air quality data

We illustrate SGFL with an application to air quality monitoring. The dataset used in this example is analyzed in Vito et al. (2008) and available on the UCI Machine Learning Repository (<https://archive.ics.uci.edu>). It contains 9358 instances of hourly averaged responses from an array of 5 metal oxide chemical sensors embedded in an Air Quality Chemical Multisensor Device. The device was located in a significantly polluted area, at road level, within an Italian city. Data were recorded from March 2004 to February 2005. Ground Truth hourly averaged concentrations for carbon monoxide (CO), Non Metanic Hydrocarbons (NMHC), Benzene (C6H6), Total Nitrogen Oxides (NOx) and Nitrogen Dioxide (NO2) were provided by a co-located reference certified analyzer. As described in Vito et al. (2008), the data show evidence of cross-sensitivity as well as of concept and sensor drift, which ultimately affects the sensors' capability to estimate pollutant concentration.

The hourly averaged measurements of the 4 target pollutants, 5 chemical sensors, and

3 meteorological variables (temperature, relative humidity, and absolute humidity) are displayed in Figure 2. For ease of visualization, variables are shifted and scaled in this figure. In the statistical analysis, all variables are centered and scaled. Missing values are ignored, i.e., only complete cases are utilized, which reduces the time series length to $T = 6930$. Correlation patterns between variables are depicted in Figure 3.

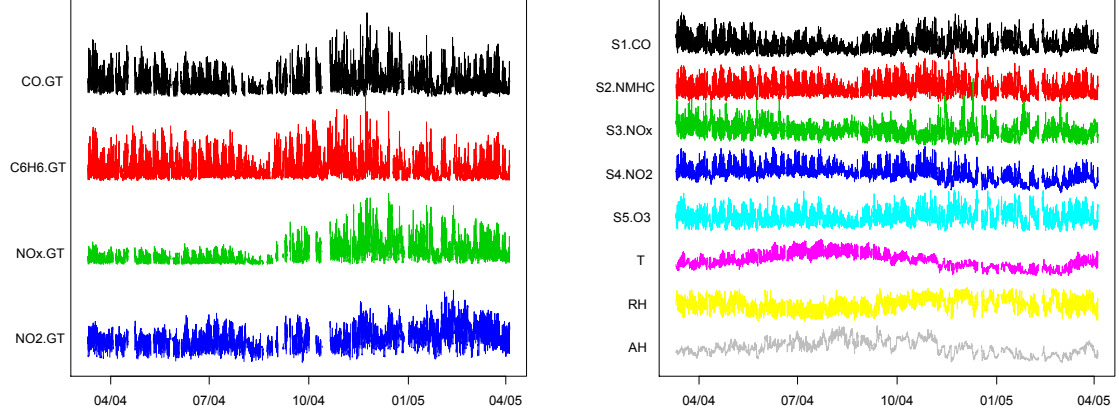


Figure 2: Air quality data. Left: pollutant levels (ground truth). Right: sensor measurements and meteorological variables. After each sensor number S1, S2, ... is the pollutant nominally targeted by this sensor.

The main goals in this application are to: (i) calibrate the sensors so that they accurately estimate the true pollutant concentrations, and (ii) determine how often the sensors must be recalibrated in order to maintain a high accuracy. Here we use SGFL in an exploratory way to determine which sensors and weather variables are predictive of the true pollutant levels, and how the regression relationship evolves over time. The relationship between the study variables is conveniently expressed as

$$y_t = A_t x_t + \varepsilon_t \quad (33)$$

where $y_t \in \mathbb{R}^d$ represents the true pollutant concentrations at time t , $x_t \in \mathbb{R}^m$ the sensor measurements and weather variables, and $A_t \in \mathbb{R}^{d \times m}$ the unknown regression coefficients with $d = 4$ and $m = 8$ or $m = 9$ if the model contains an intercept. This model can easily be recast in the form $y_t = X_t \beta_t + \varepsilon_t$ considered throughout the paper by setting $\beta_t = \text{vec}(A_t)$ (concatenate the columns of A_t) and $X_t = (x'_t) \otimes I_d$ (Kronecker product). However with this formulation the matrix $X_t \in \mathbb{R}^{d \times dm}$ becomes large and sparse, which tends to slow down calculations. For computational speed as well as user convenience, our R package **sparseGFL** has dedicated functions for both models $y_t = X_t \beta_t + \varepsilon_t$ and (33).

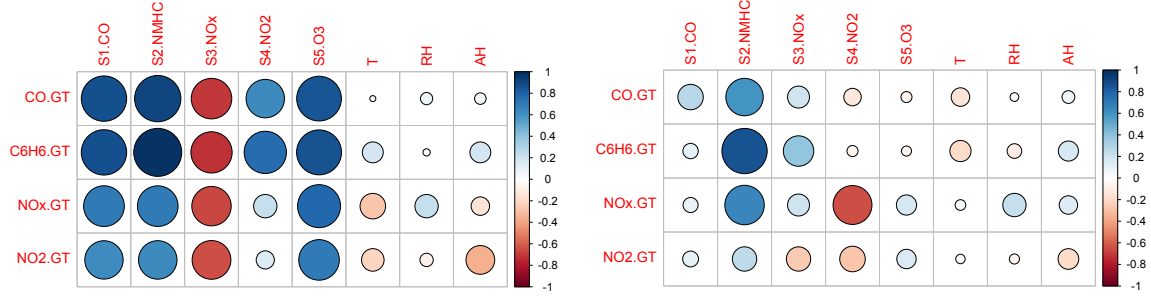


Figure 3: Air quality data: correlation between pollutant levels and predictors. Left: full correlation. Almost all sensors are strongly correlated to all true pollutant concentrations. This correlation is positive as expected for all sensors except for S3.NOx, which is surprising. Right: partial correlation. S2.NMHC is by far the strongest predictor of all pollutant levels (in equality with S4.NO2 for the target NOx. Interestingly none of the sensors is the best predictor for the pollutant it nominally targets.

Model fitting

The main model considered in our data analysis is (33) with x_t containing all sensor measurements, weather variables, plus an intercept ($m = 9$, $p = dm = 36$). For comparison, we have also examined the corresponding time-invariant model $y_t = Ax_t + \varepsilon_t$ as well as a much more complex piecewise regression model containing all sensor measurements, lagged versions thereof, weather variables, and interaction terms. (This model had $p = 156$ regression coefficients per time point for a total of about 1.08 million optimization variables.) The motivation for this model was to investigate whether exploiting sensor measurements from the recent past could enhance estimation accuracy and whether weather conditions did modulate the regression relationship between sensors and targets. Our results were inconclusive with regards to these questions and because the complex model did not decisively improve upon the main-effects-only model, we did not pursue it further. We thus focus on model (33) with $m = 9$ predictors and on the time-invariant model.

The time-invariant regression model was fitted to the data by ordinary least squares (OLS). The SGFL was solved with the hybrid algorithm for 270 couples (λ_1, λ_2) spanning several orders of magnitudes: $[10^{-4}, 1]$ for λ_1 and $[5, 200]$ for λ_2 . The total variation penalty weights w_t were set to 1. A small ridge regression penalty was added to the lasso penalty in (7) to stabilize the estimation (mixing coefficient $\alpha = 0.9$ in (35)). For each (λ_1, λ_2) , after calculating the SGFL solution $\tilde{A} = \tilde{A}(\lambda_1, \lambda_2) \in \mathbb{R}^{d \times m \times T}$, model (33) was re-estimated by OLS while preserving the zero coefficients and fusion chains of \tilde{A} : $\min_A \frac{1}{2} \sum_t \|A_t x_t - y_t\|_2^2$ subject to $(A_t)_{ij} = 0$ if $(\tilde{A}_t)_{ij} = 0$ and $A_t = \dots = A_{t+k}$ if $\tilde{A}_t = \dots = \tilde{A}_{t+k}$. This re-estimation step is common in penalized regression and serves to reduce the bias induced

by the penalty. We denote by SGFL-OLS this two-stage estimation procedure and by $\hat{A} = \hat{A}(\lambda_1, \lambda_2)$ the associated estimator.

Among the 270 SGFL-OLS solutions $\hat{A}(\lambda_1, \lambda_2)$, the “best” solution was taken to be the one for which (λ_1, λ_2) minimizes the generalized cross-validation score

$$\text{GCV}(\lambda_1, \lambda_2) = \frac{\frac{1}{T} \sum_{t=1}^T \left\| \hat{A}_t(\lambda_1, \lambda_2) x_t - y_t \right\|_2^2}{\left(1 - \frac{1}{pT} \text{df}(\hat{A}(\lambda_1, \lambda_2)) \right)^2} \quad (34)$$

where $\text{df}(\hat{A}(\lambda_1, \lambda_2))$ represents the degrees of freedom of the estimator $\hat{A}(\lambda_1, \lambda_2)$. By analogy with 1D-fused lasso regression where the (estimated) degrees of freedom are the number of nonzero fusion chains (Tibshirani et al., 2005), we define $\text{df}(\hat{A}(\lambda_1, \lambda_2))$ as $\sum_{k=1}^K \{(i, j) : (\hat{A}_{T_k}(\lambda_1, \lambda_2))_{ij} \neq 0\}$ where $C_k = \{t : T_k \leq t < T_{k+1}\}$ ($1 \leq k \leq K$) are the fusion chains associated with $\hat{A}(\lambda_1, \lambda_2)$. With this definition, one may check that $\text{df}(\hat{A}(\lambda_1, \lambda_2)) = 0$ if $\hat{A} \equiv 0$ (fully sparse, no change points) and $\text{df}(\hat{A}(\lambda_1, \lambda_2)) = pT$ if $(\hat{A}_t)_{ij} = 0$ for all (i, j, t) and $K = T$ (fully dense, all change points). Although GCV has not been studied in the specific context of SGFL, its practical efficiency and theoretical properties have been established in many contexts including closely related ones (Jansen, 2015). In our experiments we have found the GCV criterion to give more sensible results than the classic Akaike Information Criterion (AIC) and Bayes Information Criterion (BIC).

Results

Due to the close connection between partial correlation and multiple regression, the time-invariant regression estimate $\hat{A} = (YX')(XX')^{-1} \in \mathbb{R}^{4 \times 9}$ is qualitatively comparable to the partial correlation matrix of Figure 3. In model (33) with $m = 9$ predictors (sensors, weather variables, intercept), the optimal (re-estimated) SGFL solution $\hat{A}(\lambda_1, \lambda_2)$ is, according to the GCV, obtained for $\lambda_1 = 0.0064$ and $\lambda_2 = 45$. This solution has a sparsity level of 9.1% and produces a segmentation of the time range $\{1, \dots, T\}$ into $K = 18$ segments. Its overall R^2 is 93.8%.

Table 3 reports the R^2 coefficient of each fitted model for each pollutant. For the time-invariant model, this measure varies quite a bit, going from 0.756 for NO2 to 0.974 for C6H6. Given the high accuracy required in air quality monitoring, even a R^2 of 0.974 may not be acceptable for industry standards. Although the piecewise model (33) considerably improves upon the time-invariant model in terms of R^2 (8.5% overall), more sophisticated methods are required to capture the nonlinear component of the relationship between target pollutants and the sensors, e.g. neural network architectures as in Vito et al. (2008).

Table 3: Air quality data: goodness of fit (R^2) of multivariate linear regression models. The time-invariant model is fitted by ordinary least squares. The piecewise-constant model is obtained by solving the SGFL (7) for a range of values (λ_1, λ_2) and selecting the model that minimizes a generalized cross-validation criterion.

Regression model	CO	C6H6	NOx	NO2
Time-invariant	0.886	0.974	0.842	0.756
Time-varying	0.936	0.988	0.938	0.892

Figure 4 reveals a surprising acceleration in the frequency of change points between the start and the end of the observation period. This phenomenon warrants further analyses and investigations. The figure also shows the top 6 regression coefficients (by magnitude) SGFL/OLS solution. The fact that 4 out of 6 of these coefficients involve S2.NHMC as a strong predictor is in line with the findings of Figure (3). So is the fact that S4.NO2 has a fairly strong negative relationship with the level of its target NO2.GT.

5 Discussion

5.1 Summary

In this paper we have introduced the sparse group fused lasso (SGFL) as a statistical paradigm for the segmentation of high-dimensional regression models. The objective function of SGFL is designed to favor sparsity in individual regression coefficients via a lasso penalty, and to promote parsimony in the number of segments or change points via an ℓ_2 total variation penalty. To optimize this objective function, which is a nontrivial problem of nonsmooth and nonseparable convex optimization, a hybrid method was developed. This approach exploits the problem’s structure by operating at different levels (i.e. coordinate block, single fusion chain, all fusion chains, all blocks) with different optimization techniques at each level: FISTA with a novel iterative soft-thresholding technique for single blocks and fusion chains; FISTA with backtracking when optimizing over all chains; and a subgradient method to optimize over all blocks. The hybrid approach aims to identify the optimal model segmentation as early as possible and then solve the associated reduced problem –with one block of coordinates per segment instead of one block per time point. With its ability to perform local or global, aggregating or splitting iterations, the hybrid algorithm can flexibly explore the search space but also “lock in” a given model segmentation and make extremely fast progress. In our simulations, the hybrid algorithm realized significant speed gains in comparison to state-of-the-art techniques like ADMM and primal-dual methods. The speedup was particularly important in high-dimensional

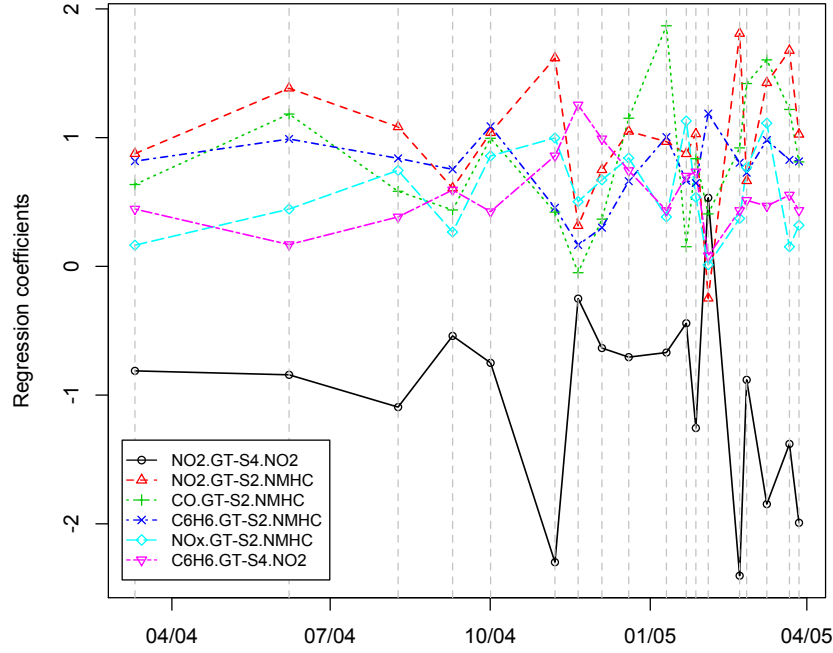


Figure 4: Air quality data: time-varying regression coefficients and model segmentation obtained by SGFL. For clarity, the piecewise-constant coefficients are represented with continuous lines rather than step functions.

situations with millions of optimization variables (30%-40% speedup in presented simulations). In addition to its computational speed, the proposed hybrid algorithm bears the advantage of not requiring any complicated selection of tuning parameters. This may help render it more accessible to non-expert users. The main parameters of the algorithm are numerical tolerances used in stopping criteria. These parameters are easily interpretable and can be set to about 10^{-6} or 10^{-7} for medium accuracy, or to 10^{-8} or 10^{-9} for high accuracy.

5.2 Extensions

Elastic net penalty

The sparse group fused lasso can be extended to encompass an *elastic net* penalty (Zou and Hastie, 2005):

$$\min_{\beta \in \mathbb{R}^{pT}} \left\{ \frac{1}{2} \sum_{t=1}^T \|y_t - X_t \beta_t\|_2^2 + \lambda_1 \sum_{t=1}^T \left(\alpha \|\beta_t\|_1 + \frac{(1-\alpha)}{2} \|\beta_t\|_2^2 \right) + \lambda_2 \sum_{t=1}^{T-1} w_t \|\beta_{t+1} - \beta_t\|_2 \right\}. \quad (35)$$

The elastic net penalty combines the lasso penalty and the (squared ℓ_2) ridge regression penalty thanks to a mixing coefficient $\alpha \in [0, 1]$ ($\alpha = 1$ corresponds to pure lasso, $\alpha = 0$ to pure ridge). This penalty seeks the “best of both worlds”, namely the sparsity-inducing effect of the lasso and the stabilization effect of ridge regression. In particular the ridge penalty can mitigate the adverse effects of high correlation among predictors in lasso. Also, from a theoretical perspective, when $\alpha < 1$, the objective function F is strictly convex and thus admits a unique minimizer.

Graph structure

The methods and results of this paper easily generalize to multivariate data observed on a general graph, of which the time chain $\{1, \dots, T\}$ is a simple example. Consider a graph structure (V, E) where V denotes a set of vertices and E denotes a set of directed or undirected edges. For example, V could be the pixels/voxels of a 2-D/3-D image while E would encode the neighborhood structure. This leads to the *graph-guided fused lasso* problem

$$\min_{\beta \in \mathbb{R}^{p(\#V)}} \left\{ \frac{1}{2} \sum_{v \in V} \|y_v - X_v \beta_v\|_2^2 + \lambda_1 \left(\alpha \sum_{v \in V} \|\beta_v\|_1 + \frac{1-\alpha}{2} \sum_{v \in V} \|\beta_v\|_2^2 \right) + \lambda_2 \sum_{(u,v) \in E} w_{uv} \|\beta_u - \beta_v\|_2 \right\}. \quad (36)$$

Loss function

For simplicity of exposition, we have developed SGFL and the hybrid optimization method in the context of time-varying linear regression. However, they are by no means restricted

to linear regression: the squared loss in the objective function (7) can be replaced by any differentiable loss function. For example, our methodology can be used for (time-varying) classification problems using exponential, logistic, or generalized smooth hinge loss functions.

5.3 Future lines of research

Several interesting directions present themselves for future research on sparse group fused lasso and the hybrid optimization scheme developed in this paper.

Pathwise implementation of SGFL

In practice, one rarely solves the SGFL for a single pair of regularization parameters (λ_1, λ_2) but rather along a path of values for these parameters. The selection of such path is in itself a nontrivial problem for two main reasons: first, the mutual dependence between λ_1 and λ_2 and second, the computation time required to fit the SGFL. More precisely, a “good” value λ_1 , e.g. one that produces a low GCV score in (34), is only good for a (typically small) range of values λ_2 and vice and versa. In addition, because of the non-negligible time required to fit the SGFL for a single couple (λ_1, λ_2) , it would be computationally very wasteful to, say, take a large lattice $\{(\lambda_1^{(i)}, \lambda_2^{(j)}) : 1 \leq i \leq n_1, 1 \leq j \leq n_2\}$, fit the SGFL for each of the $n_1 n_2$ possible (λ_1, λ_2) , and disregard bad solutions. Thus, computationally efficient methods are needed to jointly select paths of values (λ_1, λ_2) that are likely to produce good solutions.

For a given path of values for (λ_1, λ_2) , a pathwise implementation of SGFL may reduce computation time with usual tricks such as parallel computations and warm starts. But the question remains: what is the most efficient way to accomplish the pathwise implementation? Should one fix λ_1 and calculate regularization paths over λ_2 or the other way around? Should the regularization path go by decreasing order of λ_1 (sparse to dense solutions) or λ_2 (solutions with increasing numbers of change points), or by increasing order? Because SGFL does not share the nice properties of simpler problems like the fused lasso (FL), such as the monotonic inclusion of change points along regularization paths (if t is a change point in the FL solution $\beta(\lambda_2)$, it stays a change point in the FL solution $\beta(\lambda'_2)$ for all $\lambda'_2 \geq \lambda_2$), there is currently little theoretical guidance for the implementation of regularization paths. Theoretical and methodological contributions would be needed to advance this topic.

Screening rules for change points

In lasso and fused lasso regression, there exist powerful screening rules for identifying zero coefficients (lasso) or fused coefficients (fused lasso) in solutions before to start computing these solutions (Tibshirani et al., 2012; Wang et al., 2015). Such screening rules often greatly reduce the number of variables to optimize in the objective function and thus considerably speed up calculations. It would be very interesting to see if existing rules can be adapted to the more difficult problem SGFL or if novel screening rules can be devised for it.

A Proof of Theorem 2

Recall the notations of section 3.2:

$$\begin{aligned}
g(\beta_t) &= \lambda_1 \|\beta_t\|_1 + \lambda_2 w_{t-1} \|\beta_t - \hat{\beta}_{t-1}\|_2 + \lambda_2 w_t \|\beta_t - \hat{\beta}_{t+1}\|_2, \\
g_1(\beta_t) &= \lambda_1 \|\beta_t\|_1, \\
g_2(\beta_t) &= \lambda_2 w_{t-1} \|\beta_t - \hat{\beta}_{t-1}\|_2 + \lambda_2 w_t \|\beta_t - \hat{\beta}_{t+1}\|_2 + (L_t/2) \|\beta_t - z_t\|_2^2, \\
\bar{g}(\beta_t) &= g(\beta_t) + (L_t/2) \|\beta_t - z_t\|_2^2 = g_1(\beta_t) + g_2(\beta_t), \\
\gamma_n &= (L_t + (\lambda_2 w_{t-1} / \|\beta_t^n - \hat{\beta}_{t-1}\|_2) + (\lambda_2 w_t / \|\beta_t^n - \hat{\beta}_{t+1}\|_2))^{-1}, \\
\beta_t^* &= \operatorname{argmin} \bar{g} = \operatorname{prox}_{\bar{g}/L_t}(z_t), \quad r_n = \bar{g}(\beta_t^n) - \bar{g}(\beta_t^*).
\end{aligned}$$

In view of Remark 2 framing the iterative soft-thresholding scheme (21)-(22) as a proximal gradient method, we can establish the linear convergence of this scheme to $\operatorname{prox}_{\bar{g}/L_t}(z_t)$ by adapting the results of Bredies and Lorenz (2008) to a nonsmooth setting. Essentially, the proof of linear convergence in Bredies and Lorenz (2008) works by first establishing a lower bound on $\bar{g}(\beta_t^n) - \bar{g}(\beta_t^*)$, the decrease in the objective function between successive iterations of the proximal gradient method (Lemma 1). This general result shows in particular that when using sufficiently small step sizes, the proximal gradient is a descent method. After that, under the additional assumptions that g_2 is convex and that $\|\beta_t^n - \beta_t^*\|_2^2 \leq cr_n$ for some $c > 0$, the lower bound of Lemma 1 is exploited to show the exponential decay of (r_n) and the linear convergence of (β_t^n) (Proposition 2). In a third movement, the lower bound of Lemma 1 is decomposed as a Bregman-like distance term involving g_1 plus a Taylor remainder term involving g_2 . The specific nature of g_1 (ℓ_1 norm) and possible additional regularity conditions on g_2 (typically, strong convexity) are then used to establish the linear convergence result (Theorem 2). For brevity, we refer the reader to Bredies and Lorenz (2008) for the exact statement of these results.

Lemma 1 and Proposition 2 of Bredies and Lorenz (2008) posit, among other things, that the “smooth” part of the objective, g_2 in our notations, is differentiable everywhere and

has a Lipschitz-continuous gradient. In the present case, g_2 is not differentiable at $\hat{\beta}_{t-1}$ and $\hat{\beta}_{t+1}$; however it is differentiable everywhere else and its gradient is Lipschitz-continuous in a local sense. The main effort required for us is to show that Lemma 1 still holds if the points of nondifferentiability of g_2 are not on segments joining the iterates $\beta_t^n, n \geq 0$. Put differently, the iterative soft-thresholding scheme should not cross $\hat{\beta}_{t-1}$ and $\hat{\beta}_{t+1}$ on its path. This is where the requirement that $\bar{g}(\beta_t^0) < \min(\bar{g}(\hat{\beta}_{t-1}), \bar{g}(\hat{\beta}_{t+1}))$ in Theorem 2 plays a crucial part. We now proceed to adapt Lemma 1, after which we will establish the premises of Theorem 2 of Bredies and Lorenz (2008).

Adaptation of Lemma 1 of Bredies and Lorenz (2008) The main result we need prove is that

$$\forall n \in \mathbb{N}, \quad \{\hat{\beta}_{t-1}, \hat{\beta}_{t+1}\} \cap \{\alpha\beta_t^n + (1-\alpha)\beta_t^{n+1} : 0 \leq \alpha \leq 1\} = \emptyset. \quad (37)$$

Once this is established, we may follow the proof of Proposition 2 without modification. In particular, we will be in position to state that

$$\|\nabla g_2(\beta_t^n + \alpha(\beta_t^{n+1} - \beta_t^n)) - \nabla g_2(\beta_t^n)\|_2 \leq \alpha \tilde{L}_n \|\beta_t^{n+1} - \beta_t^n\|_2 \quad (38)$$

for all $n \in \mathbb{N}$ and $\alpha \in [0, 1]$, where

$$\tilde{L}_n = L_t + \frac{2\lambda_2 w_{t-1}}{\|\beta_t^n - \hat{\beta}_{t-1}\|_2} + \frac{2\lambda_2 w_t}{\|\beta_t^n - \hat{\beta}_{t+1}\|_2}.$$

Note that the left-hand side in (38) is not well defined if (37) does not hold. Combining the local Lipschitz property (38) with the step size condition $\gamma_n < 2/\tilde{L}_n$, we may go on to establish the descent property (3.5) of Bredies and Lorenz (2008):

$$\bar{g}(\beta_t^{n+1}) \leq \bar{g}(\beta_t^n) - \delta D_{\gamma_n}(\beta_t^n) \quad (39)$$

where

$$D_{\gamma_n}(\beta_t^n) = g_1(\beta_t^n) - g_1(\beta_t^{n+1}) + \nabla g_2(\beta_t^n)'(\beta_t^n - \beta_t^{n+1}) \quad \text{and} \quad \delta = 1 - \frac{\max_n \gamma_n \tilde{L}_n}{2}.$$

Lemma 1 shows that $D_{\gamma_n}(\beta_t^n) \geq \|\beta_t^n - \beta_t^{n+1}\|_2^2 / \gamma_n \geq 0$. To show the positivity of δ , note that

$$\gamma_n \tilde{L}_n = 2 - L_t \left(L_t + \frac{\lambda_2 w_{t-1}}{\|\beta_t^n - \hat{\beta}_{t-1}\|_2} + \frac{\lambda_2 w_t}{\|\beta_t^n - \hat{\beta}_{t+1}\|_2} \right)^{-1}.$$

Given the descent property of (β_n) for \bar{g} , the assumption $\bar{g}(\beta_t^0) < \min(\bar{g}(\hat{\beta}_{t-1}), \bar{g}(\hat{\beta}_{t+1}))$, and the convexity of the sublevel sets of \bar{g} , it holds that $\|\beta_t^n - \hat{\beta}_{t-1}\|_2 \geq d(\hat{\beta}_{t-1}, \{\beta_t : \bar{g}(\beta_t) \leq$

$\bar{g}(\beta_t^0)\}$ for all $n \in \mathbb{N}$; an analog inequality holds for $\hat{\beta}_{t+1}$. Denoting these positive lower bounds by m_{t-1} and m_{t+1} , we have

$$0 < \frac{1}{2} \left(1 + \frac{\lambda_2 w_{t-1}}{L_t m_{t-1}} + \frac{\lambda_2 w_t}{L_t m_{t+1}} \right)^{-1} \leq \delta \leq \frac{1}{2}. \quad (40)$$

Together, the step size condition $\gamma_n < 2/\tilde{L}_n$, descent property (39), and lower bound (40) finish to establish Lemma 1 and the precondition of Proposition 2 of Bredies and Lorenz (2008).

It remains to prove (37). We will show a weaker form of (39), namely that $\bar{g}(\beta_t^{n+1}) \leq \bar{g}(\beta_t^n)$ for all n . This inequality, combined with the convexity of \bar{g} and the assumption $\bar{g}(\beta_t^0) < \min(\bar{g}(\hat{\beta}_{t-1}), \bar{g}(\hat{\beta}_{t+1}))$, implies that $\hat{\beta}_{t-1}$ and $\hat{\beta}_{t+1}$ cannot be on a segment joining β_t^n and β_t^{n+1} . Otherwise, the convexity of \bar{g} would imply that, say, $\bar{g}(\hat{\beta}_{t-1}) \leq \max(\bar{g}(\beta_t^n), \bar{g}(\beta_t^{n+1})) \leq \bar{g}(\beta_t^n) \leq \dots \leq \bar{g}(\beta_t^0) < \bar{g}(\hat{\beta}_{t-1})$, a contradiction.

To prove the simple descent property, we start with an easy lemma stated without proof.

Lemma 1. *For all $x, y \in \mathbb{R}^p$ such that $y \neq 0_p$,*

$$\|x\|_2 \leq \|y\|_2 + \frac{y'(x-y)}{\|y\|_2} + \frac{\|x-y\|_2^2}{2\|y\|_2}.$$

Applying this lemma to $x = \beta_t - \hat{\beta}_{t\pm 1}$ and $y = \beta_t^n - \hat{\beta}_{t\pm 1}$, we deduce that for all $\beta_t \in \mathbb{R}^p$,

$$\|\beta_t - \hat{\beta}_{t-1}\|_2 \leq \|\beta_t^n - \hat{\beta}_{t-1}\|_2 + \frac{(\beta_t - \hat{\beta}_{t-1})'(\beta_t - \beta_t^n)}{\|\beta_t^n - \hat{\beta}_{t-1}\|_2} + \frac{\|\beta_t - \beta_t^n\|_2^2}{2\|\beta_t^n - \hat{\beta}_{t-1}\|_2}, \quad (41)$$

$$\|\beta_t - \hat{\beta}_{t+1}\|_2 \leq \|\beta_t^n - \hat{\beta}_{t+1}\|_2 + \frac{(\beta_t - \hat{\beta}_{t+1})'(\beta_t - \beta_t^n)}{\|\beta_t^n - \hat{\beta}_{t+1}\|_2} + \frac{\|\beta_t - \beta_t^n\|_2^2}{2\|\beta_t^n - \hat{\beta}_{t+1}\|_2}. \quad (42)$$

In addition, it is immediate that

$$\|\beta_t - z_t\|_2^2 = \|\beta_t^n - z_t\|_2^2 - 2(\beta_t^n - z_t)'(\beta_t - \beta_t^n) + \|\beta_t - \beta_t^n\|_2^2. \quad (43)$$

Multiplying (41) by $\lambda_2 w_{t-1}$, (42) by $\lambda_2 w_t$, (43) by $L_t/2$, summing these relations, and adding $g_1(\beta_t)$ on each side, we obtain

$$(g_1 + g_2)(\beta_t) \leq g_1(\beta_t) + g_2(\beta_t^n) + \nabla g_2(\beta_t^n)'(\beta_t - \beta_t^n) + \frac{1}{2\gamma_n} \|\beta_t - \beta_t^n\|_2^2. \quad (44)$$

The left-hand side of (44) is simply $\bar{g}(\beta_t)$. Also, in view of Remark 2, the minimizer of the right-hand side of (44) is $\mathcal{T}(\beta_t^n) = \beta_t^{n+1}$. Evaluating (44) at β_t^{n+1} and exploiting this

minimizing property, it follows that

$$\begin{aligned}
\bar{g}(\beta_t^{n+1}) &\leq g_1(\beta_t^{n+1}) + g_2(\beta_t^n) + \nabla g_2(\beta_t^n)'(\beta_t^{n+1} - \beta_t^n) + \frac{1}{2\gamma_n} \|\beta_t^{n+1} - \beta_t^n\|_2^2 \\
&\leq g_1(\beta_t^n) + g_2(\beta_t^n) + \nabla g_2(\beta_t^n)'(\beta_t^n - \beta_t^n) + \frac{1}{2\gamma_n} \|\beta_t^n - \beta_t^n\|_2^2 \\
&= \bar{g}(\beta_t^n).
\end{aligned} \tag{45}$$

This establishes the desired descent property.

Prerequisites of Theorem 2 of Bredies and Lorenz (2008) The distance $r_n = \bar{g}(\beta_t^n) - \bar{g}(\beta_t^*)$ to the minimum of the objective can be usefully decomposed as

$$\begin{aligned}
r_n &= R(\beta_t^n) + T(\beta_t^n) \\
R(\beta_t) &= \nabla g_2(\beta_t^*)'(\beta_t - \beta_t^*) + g_1(\beta_t) - g_1(\beta_t^*) \\
T(\beta_t) &= g_2(\beta_t) - g_2(\beta_t^*) - \nabla g_2(\beta_t^*)'(\beta_t - \beta_t^*)
\end{aligned} \tag{46}$$

where $R(\beta_t)$ is a Bregman-like distance and $T(\beta_t)$ is the remainder of the Taylor expansion of g_2 at β_t^* .

To obtain the linear convergence of (β_t^n) to β_t^* and the exponential decay of (r_n) to 0 with Theorem 2 of Bredies and Lorenz (2008), it suffices to show that

$$\|\beta_t - \beta_t^*\|_2^2 \leq c(R(\beta_t) + T(\beta_t)) \tag{47}$$

for some constant $c > 0$ and for all $\beta_t \in \mathbb{R}^p$.

Invoking the convexity of $\|\cdot\|_2$ and strong convexity of $\|\cdot\|_2^2$, one sees that $T(\beta_t) \geq (L_t/2)\|\beta_t - \beta_t^*\|_2^2$ for all β_t . Also, $R(\beta_t) \geq 0$ for all β_t (Lemma 2 of Bredies and Lorenz (2008)) so that c can be taken as $2/L_t$ in (47). \square

References

- Alaíz, C. M., Jiménez, Á. B., and Dorronsoro, J. R. (2013). Group fused lasso. In *Artificial Neural Networks and Machine Learning - ICANN 2013*, pages 66–73.
- Alewijnse, S. P. A., Buchin, K., Buchin, M., Sijben, S., and Westenberg, M. A. (2018). Model-based segmentation and classification of trajectories. *Algorithmica*, 80(8):2422–2452.
- Bai, J. (1997). Estimating multiple breaks one at a time. *Econometric Theory*, 13(3):315–352.

- Bai, J. and Perron, P. (2003). Computation and analysis of multiple structural change models. *Journal of Applied Econometrics*, 18(1):1–22.
- Barbero, A. and Sra, S. (2011). Fast newton-type methods for total variation regularization. In *Proceedings of the 28th International Conference on Machine Learning, ICML 2011*, pages 313–320.
- Basseville, M. and Nikiforov, I. V. (1993). *Detection of abrupt changes: theory and application*. Prentice Hall Information and System Sciences Series. Prentice Hall, Inc., Englewood Cliffs, NJ.
- Beck, A. and Teboulle, M. (2009). A fast iterative shrinkage-thresholding algorithm for linear inverse problems. *SIAM J. Imaging Sci.*, 2(1):183–202.
- Beer, J. C., Aizenstein, H. J., Anderson, S. J., and Krafty, R. T. (2019). Incorporating prior information with fused sparse group lasso: Application to prediction of clinical measures from neuroimages. *Biometrics*. In Press.
- Bertsekas, D. P. (2015). *Convex optimization algorithms*. Athena Scientific, Belmont, MA.
- Bleakley, K. and Vert, J.-P. (2011). The group fused lasso for multiple change-point detection. Technical Report hal-00602121.
- Boyd, S., Parikh, N., Chu, E., Peleato, B., and Eckstein, J. (2011). Distributed optimization and statistical learning via the Alternating Direction Method of Multipliers. *Found. Trends Mach. Learn.*, 3(1):1–122.
- Bredies, K. and Lorenz, D. A. (2008). Linear convergence of iterative soft-thresholding. *J. Fourier Anal. Appl.*, 14(5-6):813–837.
- Chen, J. and Chen, Z. (2008). Extended Bayesian information criteria for model selection with large model spaces. *Biometrika*, 95(3):759–771.
- Chen, X., Lin, Q., Kim, S., Carbonell, J. G., and Xing, E. P. (2012). Smoothing proximal gradient method for general structured sparse regression. *Ann. Appl. Stat.*, 6(2):719–752.
- Combettes, P. L. and Pesquet, J.-C. (2011). *Fixed-Point Algorithms for Inverse Problems in Science and Engineering*, chapter Proximal Splitting Methods in Signal Processing, pages 185–212. Springer New York, New York, NY.
- Condat, L. (2013). A primal-dual splitting method for convex optimization involving Lipschitzian, proximable and linear composite terms. *J. Optim. Theory Appl.*, 158(2):460–479.
- Friedman, J., Hastie, T., Höfling, H., and Tibshirani, R. (2007). Pathwise coordinate optimization. *Ann. Appl. Stat.*, 1(2):302–332.

- Fryzlewicz, P. (2014). Wild binary segmentation for multiple change-point detection. *Annals of Statistics*, 42(6):2243.
- Hallac, D., Nystrup, P., and Boyd, S. (2019). Greedy Gaussian segmentation of multivariate time series. *Adv. Data Anal. Classif.*, 13(3):727–751.
- Hoeffling, H. (2010). A path algorithm for the fused lasso signal approximator. *Journal of Computational and Graphical Statistics*, 19(4):984–1006.
- Jansen, M. (2015). Generalized cross validation in variable selection with and without shrinkage. *J. Statist. Plann. Inference*, 159:90–104.
- Kuhn, H. W. (1973). A note on Fermat’s problem. *Math. Programming*, 4:98–107.
- Leonardi, F. and Bühlmann, P. (2016). Computationally efficient change point detection for high-dimensional regression.
- Li, X., Mo, L., Yuan, X., and Zhang, J. (2014). Linearized alternating direction method of multipliers for sparse group and fused LASSO models. *Comput. Statist. Data Anal.*, 79:203–221.
- Li, Y. and Osher, S. (2009). Coordinate descent optimization for ℓ^1 minimization with application to compressed sensing; a greedy algorithm. *Inverse Probl. Imaging*, 3(3):487–503.
- Liu, J., Yuan, L., and Ye, J. (2010). An efficient algorithm for a class of fused lasso problems. In *Proceedings of the 16th ACM SIGKDD international conference on knowledge discovery and data mining*, KDD ’10, pages 323–332. ACM.
- Nesterov, Y. (2012). Efficiency of coordinate descent methods on huge-scale optimization problems. *SIAM J. Optim.*, 22(2):341–362.
- Nystrup, P., Madsen, H., and Lindström, E. (2017). Long memory of financial time series and hidden Markov models with time-varying parameters. *J. Forecast.*, 36(8):989–1002.
- Ohlsson, H., Ljung, L., and Boyd, S. (2010). Segmentation of ARX-models using sum-of-norms regularization. *Automatica*, 46(6):1107–1111.
- R Core Team (2019). *R: A Language and Environment for Statistical Computing*. R Foundation for Statistical Computing, Vienna, Austria.
- Ranalli, M., Lagona, F., Picone, M., and Zambianchi, E. (2018). Segmentation of sea current fields by cylindrical hidden markov models: a composite likelihood approach. *Journal of the Royal Statistical Society: Series C (Applied Statistics)*, 67(3):575–598.
- Rockafellar, R. (2015). *Convex Analysis*. Princeton Landmarks in Mathematics and Physics. Princeton University Press.

- Sanderson, C. and Curtin, R. (2016). Armadillo: a template-based C++ library for linear algebra. *Journal of Open Source Software*, 1:26.
- Saxén, J.-E., Saxén, H., and Toivonen, H. T. (2016). Identification of switching linear systems using self-organizing models with application to silicon prediction in hot metal. *Applied Soft Computing*, 47:271 – 280.
- Shor, N. Z. (1985). *Minimization methods for nondifferentiable functions*, volume 3 of *Springer Series in Computational Mathematics*. Springer-Verlag, Berlin. Translated from the Russian by K. C. Kiwiel and A. Ruszczyński.
- Songsiri, J. (2015). Learning multiple granger graphical models via group fused lasso. In *2015 10th Asian Control Conference (ASCC)*, pages 1–6.
- Tibshirani, R., Bien, J., Friedman, J., Hastie, T., Simon, N., Taylor, J., and Tibshirani, R. J. (2012). Strong rules for discarding predictors in lasso-type problems. *J. R. Stat. Soc. Ser. B. Stat. Methodol.*, 74(2):245–266.
- Tibshirani, R., Saunders, M., Rosset, S., Zhu, J., and Knight, K. (2005). Sparsity and smoothness via the fused lasso. *J. R. Stat. Soc. Ser. B Stat. Methodol.*, 67(1):91–108.
- Tibshirani, R. and Wang, P. (2007). Spatial smoothing and hot spot detection for CGH data using the fused lasso. *Biostatistics*, 9(1):18–29.
- Truong, C., Oudre, L., and Vayatis, N. (2018). A review of change point detection methods. *CoRR*, abs/1801.00718.
- Tseng, P. (2001). Convergence of a block coordinate descent method for nondifferentiable minimization. *J. Optim. Theory Appl.*, 109(3):475–494.
- Vũ, B. C. (2013). A variable metric extension of the forward-backward-forward algorithm for monotone operators. *Numer. Funct. Anal. Optim.*, 34(9):1050–1065.
- Vito, S. D., Massera, E., Piga, M., Martinotto, L., and Francia, G. D. (2008). On field calibration of an electronic nose for benzene estimation in an urban pollution monitoring scenario. *Sensors and Actuators B: Chemical*, 129(2):750 – 757.
- Wang, J., Fan, W., and Ye, J. (2015). Fused lasso screening rules via the monotonicity of subdifferentials. *IEEE Transactions on Pattern Analysis and Machine Intelligence*, 37(9):1806–1820.
- Weiszfeld, E. and Plastria, F. (2009). On the point for which the sum of the distances to n given points is minimum. *Annals of Operations Research*, 167(1):7–41.
- Wytock, M., Sra, S., and Kolter, J. Z. (2014). Fast Newton methods for the group fused lasso. In *Uncertainty in Artificial Intelligence, UAI 2014*, pages 888–897.

- Xu, Y. and Lindquist, M. (2015). Dynamic connectivity detection: an algorithm for determining functional connectivity change points in fmri data. *Frontiers in Neuroscience*, 9:285.
- Yan, M. (2018). A new primal–dual algorithm for minimizing the sum of three functions with a linear operator. *J. Sci. Comput.*, 76(3):1698–1717.
- Yao, Y.-C. (1988). Estimating the number of change-points via Schwarz’ criterion. *Statist. Probab. Lett.*, 6(3):181–189.
- Yuan, M. and Lin, Y. (2006). Model selection and estimation in regression with grouped variables. *J. R. Stat. Soc. Ser. B Stat. Methodol.*, 68(1):49–67.
- Zou, H. and Hastie, T. (2005). Regularization and variable selection via the elastic net. *J. R. Stat. Soc. Ser. B Stat. Methodol.*, 67(2):301–320.